The Zambezi River Delta Mangrove Carbon Project: A Pilot Baseline Assessment for REDD+ Reporting and Monitoring

Final Report

Prepared by:

Christina E. Stringer, Ph. D.
Carl C. Trettin, Ph. D.

Center for Forested Wetlands Research
U.S. Forest Service

Stanley J. Zarnoch, Ph. D.
Southern Research Station
U.S. Forest Service

Wenwu Tang, Ph. D.
Department of Geography and Earth Sciences
University of North Carolina- Charlotte

In Collaboration With:

World Wildlife Fund - Mozambique: Denise Nicolau, Rito Mabunda

Universidade de Eduardo Mondlane: Salomão Bandeira, Celia Macamo

National Aeronautics and Space Administration: Temilola Fatoyinbo, Marc Simard

U.S. Forest Service: Jason Ko

Mozambique Ministry of Agriculture: Joaquím Macuacua

1 September, 2014

i. Forward

This report summarizes the findings of the Zambezi River Delta Mangrove Carbon Project. Compact discs containing supporting materials, documents, and data will be provided to WWF-Mozambique, the Ministry of Agriculture, Dept. of Natural Resources Inventory, and Universidade de Eduardo Mondlane, Dept. of Biology, and they will also be made available at the Center for Forested Wetlands Research website (http://www.srs.fs.usda.gov/charleston/) in early 2015.

ii. Acknowledgements

This work was made possible by US AID support to the USFS under the US AID Mozambique Global Climate Change Sustainable Landscape Program, in collaboration with the Natural Resource Assessment Department of the Government of Mozambique. Denise Nicolau, Itelvino Cunat, and Rito Mabunda provided invaluable logistical support during the planning and implementation of field missions. Celia Macamo and Salamão Bandeira assisted prior to, and during field work, with identification of mangrove and other plant species. The staff of the Soils Lab at Universidade de Eduardo Mondlane completed all processing of soils and biomass samples. Julie Arnold and Artheera Bayles at the USFS Center for Forested Wetlands Research assisted with soil carbon analyses. The success of this project would not have been possible without the hard work and dedication of the 2012 and 2013 mission field crews: Jeremias Isaias, Damboia Cossa, Marcia Nrepo, Luis Comissario, Amisse Abel, Ezidio Cuambe, Eduardo Namalango, Joaquim Mapacare, Herculano Portraite, Dinis Chichava, Artur Titos, Jaime Matsinhe, Semo Mapai, Etelvino Fondo, Carmer de Jesus, Declerio Mucachua, and Timotio Machava.

iii. Photo Credits

All photographs contained within the report should be credited to Christina Stringer and Carl Trettin.

Contents

List of Tables

List of Figures

Acronyms

Acronym	Explanation
CEPAM	Center for Coastal and Marine Environmental Research
CIFOR	Center for International Forestry Research
DBH	Diameter at Breast Height
FAO	Food and Agriculture Organization of the United Nations
GoM	Government of Mozambique
GPS	Global Positioning System
ICE Sat/GLAS	Ice, Cloud, and Land Elevation Satellite/Geoscience Laser Altimeter System
IPCC	Intergovernmental Panel on Climate Change
MRV	Measurement, Reporting, and Verification
NAMAS	Nationally Appropriate Mitigation Strategies
NASA	National Aeronautics and Space Administration
NGO	Non-governmental Organization
NRM	National Resources Ministry (Government of Mozambique)
REDD+	Reducing Emissions from Deforestation and Forest Degradation
SDSS	Spatial Decision Support System
SRTM	Shuttle Radar Topography Mission
UEM	Universidade de Eduardo Mondlane
UNC-C	University of North Carolina-Charlotte
US AID	United States Agency for International Development
USFS	United States Forest Service
VCS	Verified Carbon Standard
WWF	World Wildlife Federation

1 Executive Summary

Mangroves are recognized for their numerous ecosystem services and functions that are critical to environmental health and human wellbeing in the regions where they occur and beyond. Although mangroves comprise only 0.7% of the world's tropical forests, they have been shown to contain globally-significant carbon pools, storing up to five times more carbon than typical upland tropical forests per area. As a result, there is interest in considering mangroves in national climate adaptation and mitigation strategies, yet little research related to climate change and carbon sequestration has been completed in mangroves, especially in Africa. WWF-Mozambique's project, *Sustainable Finance for the Protected Areas System of Mozambique 3.3 Development of a pilot project for carbon sequestration in the mangrove forests of the Zambezi Delta, Mozambique*, aims to conserve mangroves in the Zambezi River Delta through reforestation mechanisms and implementation of sustainable use and management activities with local stakeholders, financed sustainably through carbon markets. The USFS project, *The Zambezi River Delta Mangrove Carbon Project: A Pilot Baseline Assessment for REDD+ Reporting and Monitoring* is a foundational scientific component of the larger WWF effort, designed to quantify the mangrove carbon stocks.

The objectives of this project was to contribute to Mozambique's REDD+ National Program by building in-country technical capacity and measuring the soil and vegetation carbon pools in the intact mangrove stands within the Zambezi River Delta. To implement these objectives, we designed a stratified random sampling approach to inventory the carbon pools, which was implemented in collaboration with WWF – Mozambique, the Universidade de Eduardo Mondlane, and the Mozambique Department of Natural Resources Inventory, Ministry of Agriculture. Carbon pools within the mangrove forest were categorized into live and dead overstory and understory trees, ground vegetation, litter, dead wood, and soils to a depth of 2 m, thereby providing an estimate of the ecosystem carbon pool. Those pools were measured in plots that were randomly located among the five forest canopy height strata using a spatial decision support system. The sampling design also provided the basis for scaling the measurements to provide an unbiased estimate of the ecosystem carbon stocks within the Delta.

The combined carbon content in the biomass pools ranged from 99.2 Mg ha^{-1} to 341.3 Mg ha^{-1}. Live tree biomass was the dominant pool, with above-ground biomass ranging from 75.4 Mg ha^{-1} to 268.5 Mg ha^{-1}, while below-ground biomass ranged from 23.8 Mg ha^{-1} to 72.8 Mg ha^{-1}. Soil carbon was the largest pool, containing 354.7 Mg ha^{-1} to 644.9 Mg ha^{-1} and accounting for 47%-72% of the entire stock. The ecosystem carbon density among the five height classes ranged from 354.7 Mg ha^{-1} to 644.9 Mg ha^{-1}. The estimates of carbon density within height classes were integrated with the their spatial distribution and used to scale-up to the landscape level and arrive at a total carbon stock for the Zambezi River Delta mangroves of 1.4×10^7 Mg.

The project demonstrated the effective application of canopy height as the basis for stratification and forest classification, as well as the high level of precision that can be achieved with an inventory approach to quantifying carbon stocks. Throughout the course of the project, capacity building was realized through training sessions, seminars, field sampling, and laboratory analyses. The project has also provided the first comprehensive inventory of a mangrove forest in Mozambique. Accordingly, it is recommended that the data be included in the National Forest Inventory and that a subset of the plots be made permanent and established as REDD+ MRV sites. The next step to incorporate the Zambezi River Delta mangroves into a national REDD+ program should be an assessment of mangrove land cover change, due to both natural and anthropogenic causes.

2 Background

2.1 Mangrove Definition

Mangroves are salt-tolerant trees and shrubs that grow in the intertidal regions of tropical and subtropical coastlines (FAO 2007). These sites are characterized by variable salinity and tidally-driven inundation, strong winds, and anaerobic mineral and organic soils (Kathiresan and Bingham 2001). Mangroves adapted to these conditions by developing unique structural, morphological, and reproductive adaptations, including aerial root systems, salt-extracting leaves, and viviparous water-dispersed propagules (Krauss, et al. 2008,Hogarth 2007).

2.2 Mangrove Distribution

There are 55 species of mangroves occurring in the tropical and subtropical regions of 118 countries (Hogarth 2007). The boundary for mangrove latitudinal distribution is typically delineated by the location of the 20° C isotherm of surface seawater in the winter months (Figure 2.1) (Hogarth 2007,Giri, et al. 2011). The most recent global estimate reports that there was 137,760 km^2 of mangrove area in 2000 (Giri, et al. 2011).

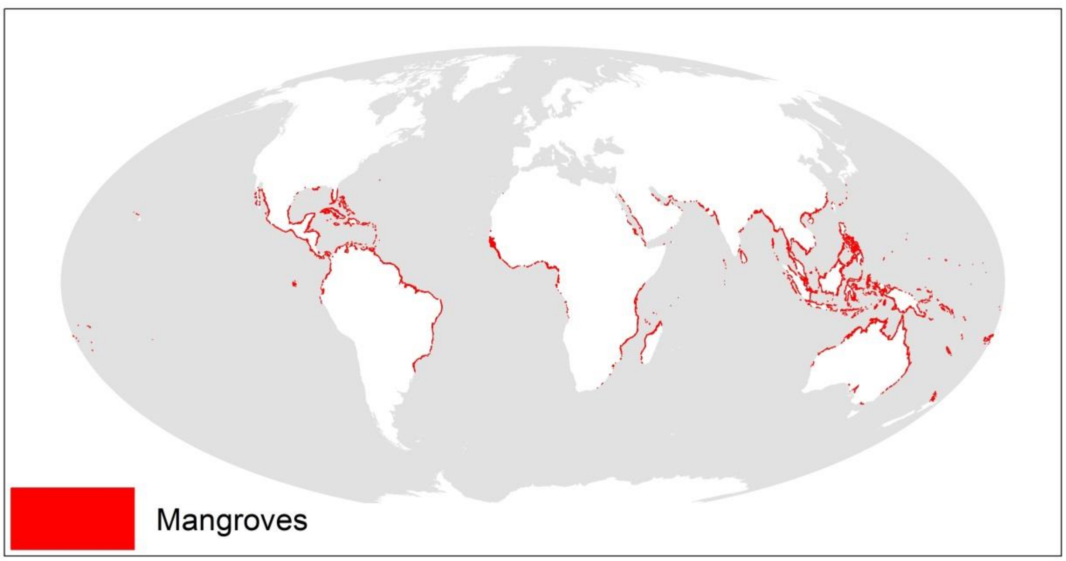

Figure 2.1. Worldwide mangrove distribution (from Giri, et al. 2011).

2.3 Mangrove Management Incentives

Deforestation and forest degradation constitute the second largest anthropogenic source of carbon dioxide to the atmosphere, after fossil fuel combustion, comprising 8-20% of anthropogenic emissions (IPCC 2013,van der Werf, et al. 2009). International programs that aim to reduce these emissions are being considered as a viable option for reducing anthropogenic greenhouse-gas emissions (Gullison, et al. 2007).

These programs exist as both compliance schemes and voluntary programs. Compliance markets are created and regulated by mandatory national, regional, or international carbon reduction regimes (e.g., emissions trading under the Kyoto Protocol and the European Union

Emissions Trading Scheme) (Kollmuss, et al. 2008). The voluntary carbon market functions separately, enabling businesses, governments, NGOs, and even individuals, to offset their emissions through the purchase of offsets created in either market. There are many greenhouse gas programs available for the voluntary carbon market, the largest of which is the Verified Carbon Standard (VCS), founded in 2005. These programs are the mechanisms necessary for projects to certify they are actively reducing emissions (Kollmuss, et al. 2008).

One mechanism that has come to the forefront of the carbon market is the UN's Reducing Emissions from Deforestation and Forest Degradation (REDD+). Since its implementation in 2008, REDD+ has become a primary focus of policy makers and organizations in their efforts to mitigate climate change (Adame, et al. 2013,Murdiyarso, et al. 2012). The REDD+ program proposes the provision of financial incentives to help developing countries not only reduce deforestation and degradation rates, but also build capacity for conservation, sustainable forest management, and even enhancement of forest carbon stocks (UN-REDD 2011).

The REDD+ program preparations have focused on terrestrial forests. A recent study showing that mangrove forests contribute up to 10% of total global deforestation emissions, despite covering just 0.7% of tropical forest area (Donato, et al. 2011), has sparked considerable discussion about the importance of including mangroves in REDD+ programs. Despite the fact that inclusion of mangroves in REDD+ programs is supported by many organizations, including the United Nations Development Program, there are few REDD+ mangrove projects in preparation at a national or sub-national scale (King 2012).

There are several barriers to the inclusion of mangroves in REDD+ programs. While a multitude of methodologies exist for terrestrial forests, there is a lack of appropriate certification methodologies for mangroves. Additionally, the administration of mangroves and their associated resources is often complicated. Mangrove management is rarely covered by one specific national policy, with numerous policies covering the various benefits provided (King 2012). A key part of REDD+ preparations is the assessment of deforestation rates to establish baselines for future activities. However, few countries have included mangroves in national baseline inventories or ongoing monitoring, reporting and verification (MRV) systems, meaning that a better understanding of mangrove deforestation rates is critical for efficient inclusion in REDD+ programs (King 2012).

2.4 Mangrove Carbon

Mangrove ecosystems provide many valuable ecosystem goods and services to coastal areas, including shoreline stabilization and fish hatchery habitat. Mangroves have also been recognized for their role in the global carbon cycle. Mangroves are one of the most carbon-rich forest types in the tropics due largely to the carbon accumulation in soils (Donato, et al. 2011). Sediments are the primary carbon pool in mangroves, regardless of tree biomass, and can store as much as three times more carbon than soils in terrestrial forests (Donato, et al. 2011,Kauffman, et al. 2011). Knowledge about mangrove carbon dynamics has improved in recent years, but there are still significant uncertainties about fluxes and the mechanisms for retaining C in the sediments that need further research (Kristensen, et al. 2008).

2.5 Assessment of Carbon Pools

Forest carbon pools should be determined using accepted inventory methodologies. Those methods require adaptation to address the unique mangrove environment (e.g., tidal inundations and aerial root systems). The sampling design for this project is based on protocols developed by CIFOR and USFS (Kauffman and Donato 2012). This protocol was developed based on forest inventory methodologies and first-applied in Indo-Pacific mangrove forests. The intent in its application for this project is to (a) utilize an established protocol to facilitate comparison with other projects, and (b) to assess whether the protocol needs to be adjusted for use in African mangrove forests. A total of 10 carbon pools are either measured or estimated, comprising above and below-ground biomass of live and dead plants and soil to a depth of 2 m (Table 2.1). These carbon pools are then integrated to provide a measure of the ecosystem carbon stock.

Table 2.1. Carbon pools reported in this inventory and a brief explanation of the evaluation approach.

Carbon Pool	Methodology
Above-Ground Biomass	
Overstory (> 5 cm DBH)	Biomass values calculated using allometric equations based on species' wood density and tree DBH field measurements
Understory (< 5 cm DBH)	Biomass Values calculated using allometric equations based on species' wood density and tree DBH field measurements
Ground Vegetation	Biomass, sampled in microplots
Wood Debris	Line-intercept method, mass reported in size classes.
Litter	Biomass, sampled in microplots
Standing Dead Tree (> 5 cm DBH)	Biomass values calculated using allometric equations dependent on extent of decay, and wood density
Below-Ground Biomass	
Overstory (> 5 cm DBH)	Biomass values calculated using allometric equations based on species' wood density and tree DBH field measurements
Understory (< 5 cm DBH)	Biomas values calculated using allometric equations based on species' wood density and tree DBH field measurements
Dead Standing Tree (> 5 cm DBH)	Biomass values calculated using allometric equations dependent on extent of decay, and wood density
Soils	Soil sampled at 6 depths to represent the soil to 2 m below the surface. Carbon mass based on measures of bulk density and C concentration.

3 Introduction

3.1 Overview of Mozambican Mangroves

Africa contains approximately 20% of the mangroves in the world (Giri, et al. 2011). Within Africa, Mozambique has the second largest mangrove cover area after Nigeria (Fatoyinbo and Simard 2013). Globally, Mozambique ranks 13th in mangrove coverage; equivalent to approximately 2.3% of the global mangrove forest area (Giri, et al. 2011). Estimates of Mozambican mangrove area vary (Table 3.1), most likely due to variation in data sources and analytical methodologies.

Table 3.1. Estimates of Mozambique's mangrove area (ha) and year of assessment.

Mangrove Area (ha)	Year	Source
408,079	1972	Saket and Matusse, 1994
396,080	1990	Saket and Matusse, 1994
392,749	1997	FAO, 2007
290,900	2005	Fatoyinbo et al., 2008
368,000	2009	Min. Coord. Env. Affairs, 2009
318,851	2011	Giri et al., 2011
305,400	2013	Fatoyinbo and Simard, 2013

Mangroves occur along the entire length of the 2,770 km Mozambican coastline, but are concentrated in the northern and central regions (Figure 3.1). In the southern portions of the coast, mangroves occur in the Morrumbene estuary, Inhambane Bay, the Bay of Maputo, and Inhaca Island (Chevallier 2013). In northern Mozambique, mangroves are present in Lumbo, Mecúfi, Ibo Island, and Pemba Bay (Barbosa, et al. 2001). The largest extent of mangroves is in central Mozambique, and includes coverages in the Zambezi, Púngue, Save, and Búzi River Deltas (Chevallier 2013). The Zambezi River Delta mangrove extends for 180 km along the coast and inland approximately 50 km, making it the second largest continuous mangrove habitats in Africa (Barbosa, et al. 2001).

There are 9 species of mangroves that occur in the East Africa eco-region. The 4 most common species are *Rhizophora mucronata* Lam., *Ceriops tagal* (Per.) C.B. Robinson, *Bruguiera gymnorrhiza* (L.) Lam., and *Avicennia marina* (Forsskk.) Vierh.. Additional species are *Sonneratia alba* Smith, *Heritiera littoralis* Alton, *Xylocarpus granatum* Koenig, *Lumnitzera racemosa* Wild., and *Avicennia officinalis* L. (Taylor, et al. 2003). Madagascar is the only country in East Africa to be home to all 9 species. Mozambican mangroves consist of 8 of the species, all but *A. officinalis*, and they all are reported in the Zambezi River Delta (Beilfuss, et al. 2001). *Pemphis acidula* Forst is sometimes cited as a ninth species occurring in Mozambique (Barbosa, et al. 2001), however this is considered by others as an associate species, rather than a true mangrove tree (Beentje and Bandeira 2007).

The majority of research and investigation on mangroves has taken place in areas around Maputo Bay, particularly Inhaca Island (Bandeira, et al. 2002). The mangrove research performed in these southern areas has focused on mangrove distribution and evaluation of the wide variety of associated ecosystem goods and services (Barbosa, et al. 2001,Bandeira, et al. 2002,Hatton and Couto 1992). While the functions of mangroves in Mozambique may be analogous to other areas (e.g., storm protection and fishery nurseries), the associated goods and services are particularly valuable given the dependence of the communities on the forests (Republic of Mozambique 2009). Locals harvest from mangroves for use in building materials for homes and boats, firewood, fencing, and fish traps (Barbosa, et al. 2001). The Zambezi River Delta's mangroves not only play a key role in sustaining the livelihoods of the nearly 200,000 people living in the region, but they are particularly important to Mozambique's economy as they support the shrimp fisheries of the Sofala Bank, a key export sector (US$114M, 14% of total exports in 2002) (WWF 2011).

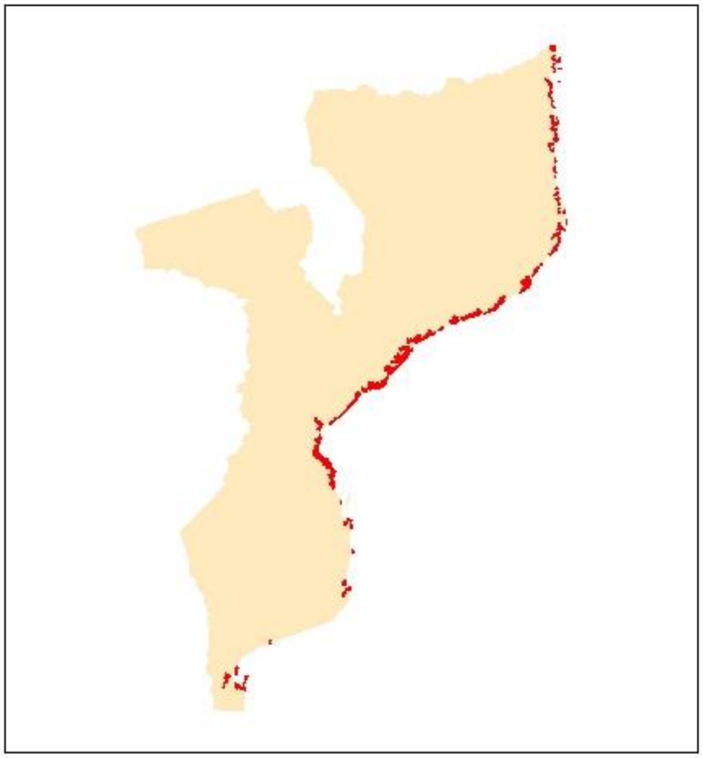

Figure 3.1. Mozambique mangrove distribution (from Giri, et al. 2011).

Mangrove investigations in other areas of Mozambique have focused on its destruction and deforestation. Mangrove decline has been reported in all coastal regions of Mozambique (Ferreira, et al. 2009,Fatoyinbo, et al. 2008,Bandeira, et al. 2009). The trend is particularly evident in the Zambezi River Delta, where a 50% decrease in mangrove coverage has been reported (Fatoyinbo, et al. 2008), particularly in the region around Chinde (Timberlake 2000). However, that estimate of loss was based on analyses of remote sensing data, was not ground-validated and it is much larger than other reports; hence it should be interpreted judiciously. Correspondingly, the decline in mangroves is not as evident in the trans-boundary area further to the north (Ferreira, et al. 2009), suggesting differences in land use and disturbance patterns along the Mozambique coast.

Despite being the most extensive area of mangrove habitat in Mozambique, the Zambezi River Delta mangroves have not been thoroughly investigated, most likely due to accessibility issues associated with the remote location. Environmental studies associated with the Delta have not been mangrove-focused, but rather focus on sustainable management of the Cahora Bassa Dam and associated impacts on water (Beilfuss and Santos 2001) and sediment (Davies, et al. 2000) delivery.

3.2 Project Objectives

The vision of the WWF project entitled *Sustainable Finance for the Protected Areas System of Mozambique 3.3 Development of a pilot project for carbon sequestration in the mangrove forests of the Zambezi Delta, Mozambique* is to develop a replicable mechanism to finance and carry out conservation and coastal community development activities based on marketing mangrove carbon sequestration. The WWF project goal is to provide the basis to conserve mangroves and habitat in the Zambezi River Delta by reforestation mechanisms and implementing sustainable use and management activities with local stakeholders, financed sustainably through carbon markets or conservation easements.

This work, “A Carbon Inventory of Mangrove Forests in the Zambezi River Delta,” is a component of US AID support to the USFS under the US AID Mozambique Global Climate Change Sustainable Landscape Program. The goal of the USAID Sustainable Landscape Program is to assist in the conservation of tropical forests by helping countries engage in REDD+, a policy approach designed to curb deforestation and related GHG emissions. REDD+ policy frameworks are rapidly emerging, but for many countries, just preparing to participate is a challenge.

In Mozambique, as in much of the developing world, establishing sustainable methodologies and systems for measuring and monitoring carbon stocks, as well as protecting natural resources from deforestation and degradation, is a priority. Furthering the understanding of national carbon stocks, like those in mangroves, will help the countries better prioritize their national REDD+ strategy, preparation, and activities. The USFS work in the Zambezi aims to address these knowledge and capacity gaps in Mozambique as well as other African countries with significant areas of mangrove forests.

The purpose of the USFS project was to define the carbon pools within the Zambezi River Delta and to contribute to methodological development of a REDD+ mangrove carbon methodology that measures and monitors the soil carbon component (WWF 2011). Considerations of deforestation rates and carbon pools in disturbed sites were beyond the scope of the current project. The specific objectives were as follows:

1) Contribute to the development of Mozambique’s REDD+ program by providing policy-relevant information necessary to establish baseline for REDD+ and other climate change mitigation activities (e.g., Nationally Appropriate Mitigation Strategies – NAMAS) for mangrove forests.

2) Build capacity in Mozambique for climate change mitigation (and adaptation) programs, specifically:

a. Demonstrate methodologies for conducting a carbon inventory;

b. Establish Monitoring, Reporting and Verification (MRV) pilot sites in mangrove forests and associated data management systems;

c. Provide opportunities for training (graduate students and staff).

3) Measure the carbon contained within the vegetation and soil of mangrove forests of the Zambezi River Delta;

a. Contribute to the development of internationally recognized methodologies for measuring mangrove ecosystem carbon stocks;

b. Contribute to the development of internationally recognized classification system for mangrove forests.

This Project was funded by USAID-Mozambique. Work to meet these objectives has been completed through collaboration of several entities (Table 3.2). WWF, as the project coordinator, brought USFS, UEM, and GoM into the project and facilitated all coordination between the various institutions. The USFS, in turn, cooperated with UNC-C and NASA to accomplish specific tasks related to inventory design.

Table 3.2. List of project entities and associated roles.

Project Partner	Role
WWF-Mozambique	Project coordinator- organize functions between collaborating institutions and support field, laboratory, and analytical activities
US AID	Sponsors USFS project involvement
USFS	Technical advisor- provides the scientific leadership for the carbon inventory, specific to the field sampling, analyses, and reporting
UEM	Project facilitator- UEM Biology, Geography, and Forestry Departments provide scientific and institutional support, including students for fieldwork implementation and basic laboratory facilities for processing and managing soil and wood samples.
GoM	Implementation- The Ministry of Agriculture, Dept. of Natural Resources Inventory is implementing the national MRV capabilities. Accordingly, the project data will be incorporated into their databases to support future assessments.
UNC – C	Develop Spatial Decision Support System for inventory design and implementation; statistical analyses.
NASA	Provision of remote sensing data.

4 Project Setting

4.1 Hydrogeomorphic Setting

The Zambezi River is the fourth-largest river system in Africa, with a length of 2,574 km and a catchment area of 1.37 million km^2, draining portions of 7 countries (World Bank, 2010). The river basin is commonly divided into three geographical sections: the Upper, the section of river between the headwaters and Victoria Falls; the Middle, the basin drained by the length between Victoria Falls and Cahora Bassa Dam; and Lower Zambezi, encompassing the extent of the river from the Cahorra Bassa Dam to the Zambezi River Delta, where it enters the Indian Ocean.

The Upper Zambezi is characterized by broad floodplains with small, scattered swamps, all set in a very flat landscape (Timberlake 1998). The Middle Zambezi can be characterized as a regulated river, due to the presence of the Kariba and Cahora Bassa Dams, running through broad valleys and gorges, with limited floodplains. In contrast, the Lower Zambezi is broad, comprised of many anastomosing channels and constantly shifting sandbanks, with a complex mosaic of associated forested wetlands and marshes (Davies, et al. 2000).

The Zambezi River Delta forms a triangle of approximately 12,000 km^2 (Beilfuss, et al. 2001). The much larger floodplain starts at the confluence of the Zambezi and Shire rivers (S 17° 41' 40'' E 35° 19' 21'') and extends 120 km downstream to the Indian Ocean. It also extends 200 km southwest-northeast along the coastline, from the Cuacua River (S 17° 53'12'' E 36° 52' 52''), in the Province of Zambezia, down to the Zuni River Delta (S 19° 10' 47'' E 35° 37' 43''), in Sofala Province.

Figure 4.1. The Zambezi River Delta region and its position on the Mozambican coast.

Within the Zambezi River Delta, the freshwater, forested floodplain transitions to tidally-influenced estuarine mud flats and raised beaches. The estuarine mud flats are dark, clayey alluvium of marine origin, rich in organic matter (Beilfuss, et al. 2001). The Zambezi River Delta is the second-largest wetland of the entire basin and the most diverse in terms of habitats, yet it is considered the least known biologically (Timberlake 1998).

The water levels in the Zambezi River Delta are reflective of the cumulative runoff patterns in the upstream sub-basins, with an estimated water volume of 108 x 10^9 m^3 reaching the Delta on an annual basis (Beilfuss and Santos 2001). The tidal regime in the Delta is semi-diurnal, with a spring tide maximum tidal amplitude of 4.1 m (Beilfuss and Santos 2001,Coleman 2004). This tidal range is the largest in Mozambique and in the dry season tidal influence is visible for up to 80 km upstream (Beilfuss and Santos 2001). Runoff patterns in the Zambezi River Delta are primarily a function of regulated outflows from the Cahora Bassa Dam, flashy runoff from the Mozambique plateau, and partially regulated Shire River inflows (Beilfuss and Santos 2001). The changes in runoff and flow patterns associated with the dam operations have affected the flooding regime in the Delta, with flows rarely inundating the floodplains on both the north and south banks, shifting the Delta hydrologic regime from a flood-driven system to a rainfall-driven system (Beilfuss and Santos 2001).

4.2 Climate

The climate of Mozambique is tropical, with two distinct seasons: a dry winter season from April to October and a wet summer season from October to March (Barbosa, et al. 2001,Hoguane 2007). The mean annual precipitation ranges from 1,000 mm at the most upstream regions of the Delta to more than 1,400 mm along the coast, with considerable inter-annual variation (Bento, et al. 2007). Eighty-five percent of the rain falls from mid-November to late March (Tweddle 2013). Mean monthly temperatures ranges from 27°C in June to a maximum of 37°C in October (Tweddle 2013).

The Zambezi River Delta is vulnerable to tropical storm activity. Cyclones cause torrential rains that can occur in any month from December to March and cause widespread local flooding (Beilfuss and Santos 2001). There was an average of 5.6 tropical storm (e.g., hurricanes, cyclones) strikes every 10 years from 1950 to 1999 (Beilfuss, et al. 2001). In addition to flooding, particularly severe storm events have been documented to affect mangrove forest structure, especially evident in *A. marina* stands, where strong winds damage tree crowns (Beilfuss, et al. 2001).

4.3 Vegetation

The Zambezi River Delta is a vegetative mixture of woodlands, savanna, grasslands, mangroves, and coastal dunes, with a mosaic of wetlands (Beilfuss, et al. 2001, World Bank 2010). Woody communities and savannas are dominated by Acacia and palms. Grasslands include swamp mosaics with areas of phragmites and papyrus (Beilfuss, et al. 2001). The coastal dunes consist of thickets and woodlands on sandy ridges, with pockets of coconut groves (Beilfuss, et al. 2001).

Zambezi River Delta mangrove communities occur on saline mudflats within the coastal estuary. There are 8 mangrove species present in the Delta, representing all of species reported to be in Mozambique: *S. alba*, *A. marina*, *R. mucronata*, *C. tagal*, *B. gymnorrhiza*, *L. racemosa*, *H. littoralis*, and *X. granatum*. Mangrove associate species tend to occur in higher elevation areas with less water inundation (Vilankulos and Marquez 2000). Major associates include *Guettarda speciosa*, *Hibiscus tiliaceous*, and the large fern *Achrostichum aureum* (Beilfuss, et al. 2001, Barbosa 2001). Thickets of *Barringtonia racemosa*, another associate, also occur along the most upstream reaches of tidal influence within the estuary (Beilfuss, et al. 2001).

The distribution and composition of mangroves are dynamic and directly related to geomorphological changes occurring as a function of coastal erosion and sedimentation processes (Smith 1992,Moll and Werger 1978). The geomorphology of the Delta is heavily affected by upstream activities and water flows, especially the operation of the Kariba and Cahora Bassa Dams. The dams not only lessen fresh-water discharge to the Delta, but also diminish sediment transport by up to 70%, resulting in coastal zone erosion and a reduction of sediment-maintained habitats, including mangroves (Davies, et al. 2000). Additionally, the Delta is subject to frequent storms that cause geomorphic changes and can also directly damage tree stands (Beilfuss, et al. 2001).

5 Methods

5.1 Inventory Design

The project area is the mangrove forest within the Zambezi River Delta (Fig. 5.1). This area was selected by WWF because it contains a large proportion of the mangroves in Mozambique and it includes the mangroves within the Marromeu Reserve. The project area includes approximately 30,267 ha of mangrove forest, distributed along the north and south sides of the river, as delineated by Fatoyinbo and Simard (2013).

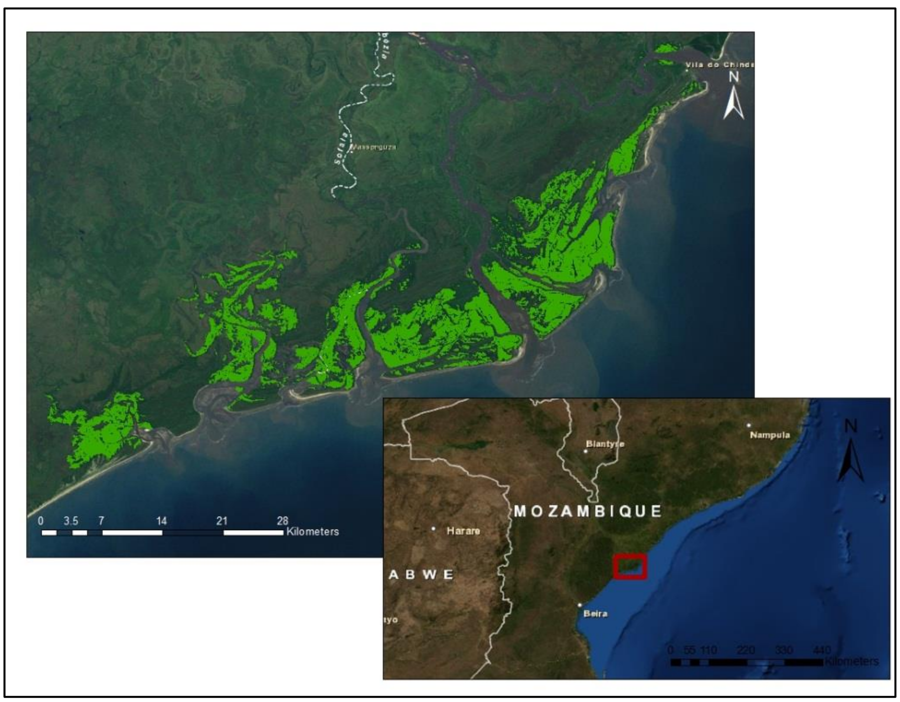

Figure 5.1. Extent of mangrove area within the Zambezi River Delta considered for this inventory, represented by the bright green shading (Fatoyinbo and Simard, 2013).

A stratified random sampling design can add efficiency and accuracy to the assessment if the strata have a functional relationship with the variable(s) being measured. Accordingly, given the size and complexity of the Zambezi River Delta, utilizing such a sampling approach is highly desirable. The first sampling mission (2012) utilized a classification that represented four forest types based on dominant mangrove species through spectral analyses of Landsat data (Rafael, et al. 2011). Analyses of the field data collected from 12 plots indicated that this basis for stratifying the sampling was not effective because the species classification did not reflect the measured species composition of the forest; hence the basis for the stratification was not supported. Accordingly, an alternative approach was deemed necessary if a stratified sampling design was to be employed.

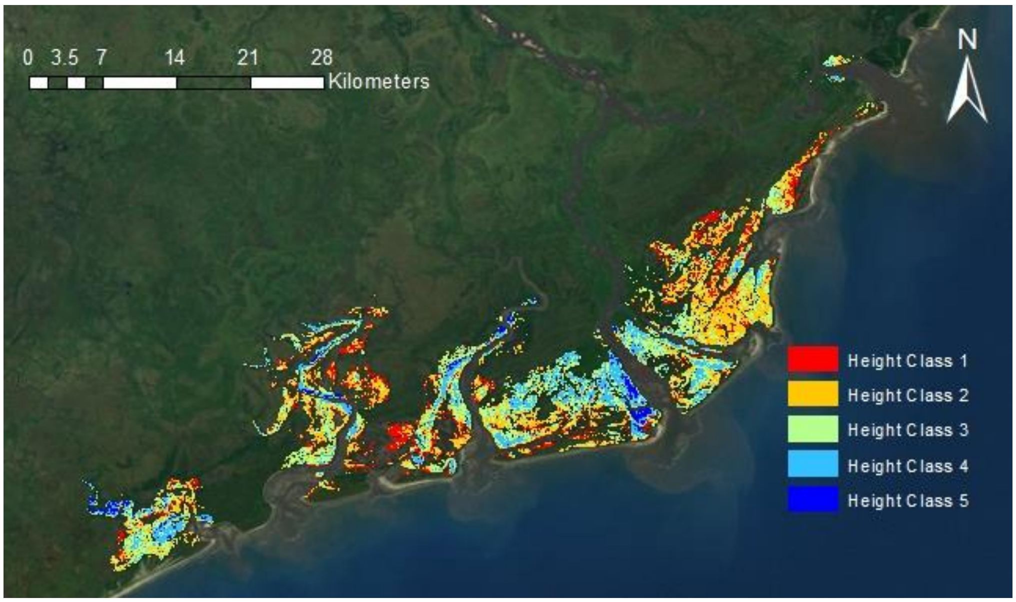

Figure 5.2. Distribution of mangrove canopy height class in the Zambezi River Delta. Canopy height data obtained from Fatoyinbo and Simard (2013). The associated height range for each class is shown in Table 5.1.

Using Ice, Cloud, and land Elevation Satellite / Geoscience Laser Altimeter System (ICE Sat/GLAS) and the Shuttle Radar Topography Mission (SRTM) data, Fatoyinbo and Simard (2013) estimated canopy height and associated above-ground forest biomass for African mangroves. Since canopy height is functionally related to biomass, a classification system based on stand structure (i.e., height) is functionally relevant to the inventory objectives. We obtained the calculated canopy height data from Dr. T.E. Fatoyinbo at NASA and worked with colleagues at UNC-Charlotte to analyze the data. Five canopy height classes were distinguished within the Zambezi River Delta (Figure 5.2; Table 5.1) (Tang, et al. 2013). These height classes were based on the distribution of canopy height among mangrove pixels (Figure 5.3).

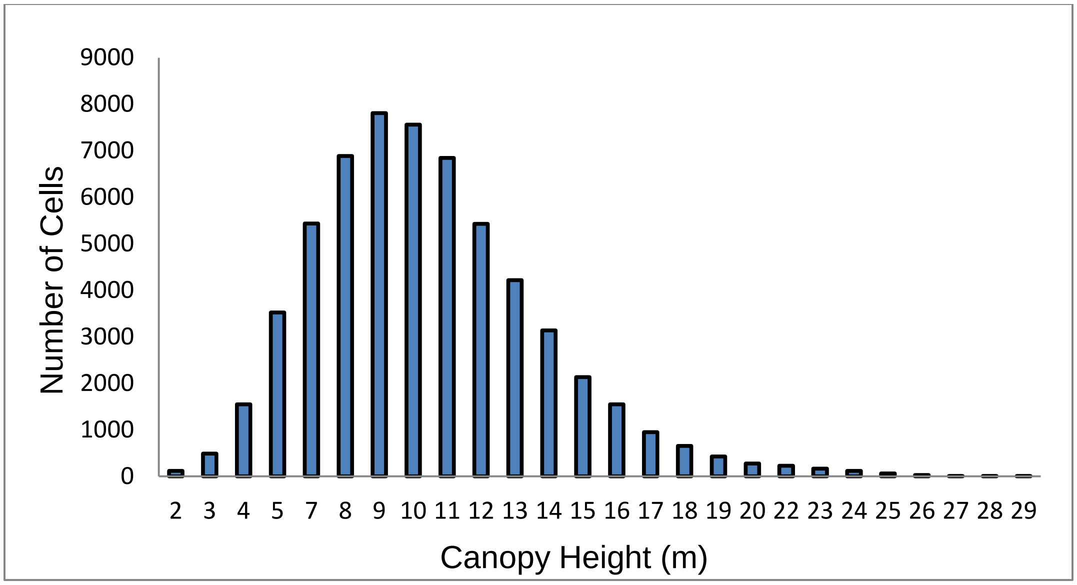

Figure 5.3. Distribution of pixel (cells) canopy height values, as determined by analysis of SRTM data (data from T.E. Fatoyinbo, NASA).

Table 5.1. Mangrove canopy height classes delineated through analysis of SRTM data (Tang, et al. 2013).

Class ID	Height (m)
1	2 - 6.9
2	7 - 9.9
3	10 - 12.9
4	13 - 17.9
5	18 - 29

The sampling approach utilizes subplots nested within the plot which provide a basis for measurement of within plot variability. The purpose of the subplots is to accommodate inherent spatial variation within the plot that is representing the mangrove stand. The subplot layout used was identical for 2012 and 2013, and was based upon protocols presented in Kauffman and Donato (2012). Each subplot consisted of a 7 m radius circle for sampling trees with a diameter at breast height (DBH) greater than 5 cm, with a nested 2 m radius circle for sampling trees with a DBH smaller than 5 cm (Figure 5.4). Four transects 12 m in length were established in each subplot to assess wood debris. Herbaceous understory and litter were measured in frames along transects. A soil core was also extracted within 2 - 3 m of the subplot center.

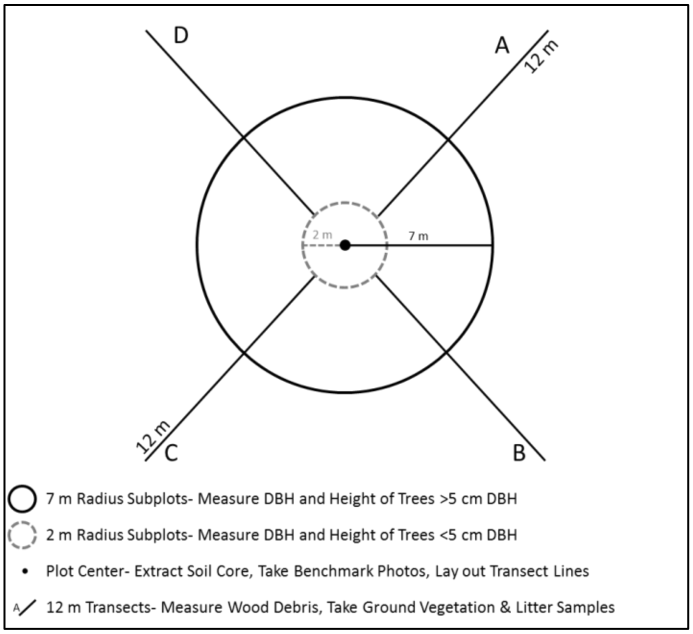

Figure 5.4. Subplot design used in the 2012 and 2013 field missions, based on Kauffman and Donato (2012). DBH represents the tree diameter at breast height.

The 2012 field mission used six subplots evenly spaced 11 m apart along a central axis 125 m in length (Figure 5.5). We sampled 12 plots in 2012: 3 replicates within each of the 4 mangrove types delineated by Rafael, et al. (2011). Forest stand structure data (i.e., basal area) from that mission was used not only to determine the number of additional plots necessary to achieve an accurate characterization of the Zambezi mangroves, but also to assess the efficiency of the sampling design. Using statistical methods, it was determined that 33-47 plots, in addition to the 12 sampled in 2012, be sampled in 2013 (Tang, et al. 2013). We chose the middle of that range, making our 2013 sampling goal 42 plots.

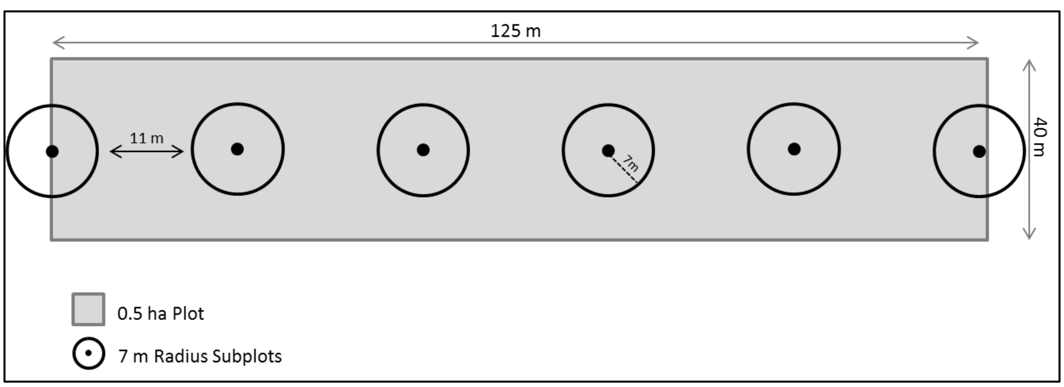

Figure 5.5. Rectangular plot layout with six subplots used in 2012 field mission (after Kauffman and Donato 2012). This plot design is best suited for sampling sites to accommodate a strong gradient.

Prior to the 2013 mission, we assessed whether the number of subplots could be reduced without sacrificing information about the variance of tree diameter and basal area. We applied

Kolgorov-Smirnov statistical analyses to the 2012 data to evaluate the smallest number of subplots that could be sampled to achieve statistically-acceptable results. There was no statistically-significant difference between empirical distributions of estimates based on 5 and 6 plots (Figure 5.6) (Tang, et al. 2013).

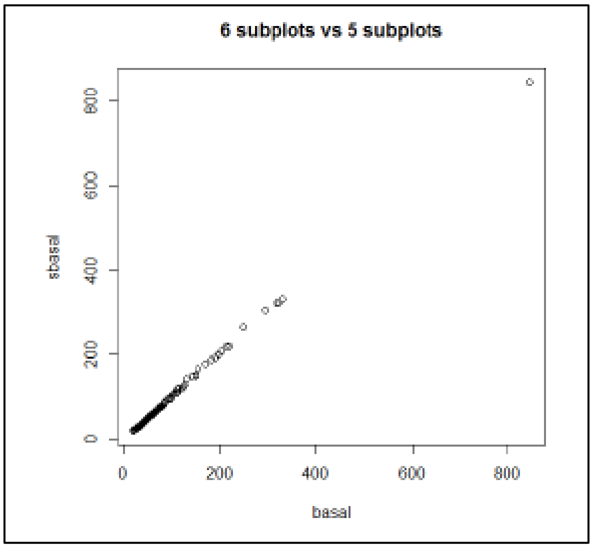

Figure 5.6. Plot showing differences of empirical distributions of estimates based on 5 and 6 subplots (Tang, et al. 2013).

Accordingly, 5 subplots were prescribed for the 2013 mission; thereby also providing gains in operational efficiency. We configured the subplots into a cross arrangement, creating a square plot rather than the rectangular plot used in 2012 (Figure 5.7). This arrangement of subplots was more suitable for our sampling design, as it approximates the shape of the remote sensing pixel, the foundation of our classification scheme. The rectangular plot shape used in 2012 is best suited toward studies where interest lies in changes in mangrove structure or character along a defined gradient (e.g., surface water salinity).

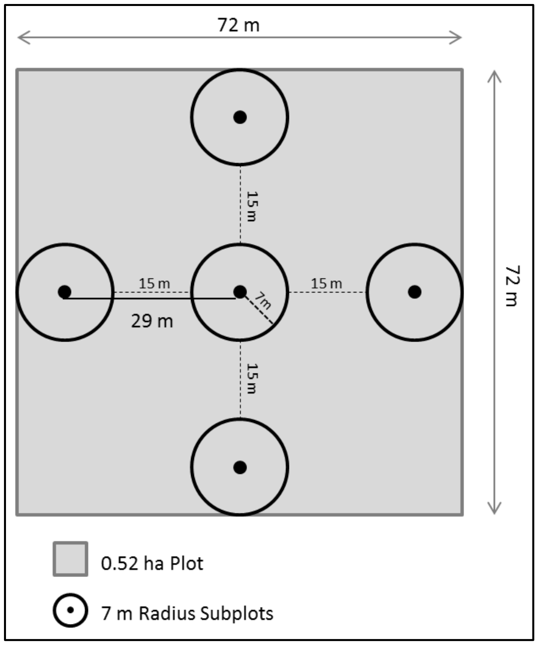

Figure 5.7. Square plot design with 5 subplots used in the 2013 field mission.

5.2 Spatial Decision Support System

Planning for the 2013 field mission included development of a Spatial Decision Support System (SDSS) that provided the framework for detailed logistical planning and field mission implementation (Tang et al., 2013). The SDSS was used to identify camping and plot locations, providing randomization of site selection and the ability to consider various logistical constraints. The design parameters were as follows:

a) Stratified sampling within the delineated area of mangroves within the Zambezi River Delta, plots must be located within uniform areas of the strata which was defined as minimum of 4 contiguous pixels in the a height class;

b) The focus of the 2013 mission will be on the southern portion of the Delta;

c) The field work will be conducted from field (i.e., “fly”) camps; that must be located near an existing village;

d) The working radius from the field camp should not exceed 8 km, perhaps less (an efficiency, safety and cost constraint)

e) Access to the field plots will be from streams, and the crew should not traverse more than 1 km from the river to establish the plot (an efficiency and safety constraint);

Data input into the SDSS included spatial layers containing village location and stream channel boundaries[1], as well as the canopy height class for each pixel. Potential plot locations were

[1] These data layers were generated from ocular interpretation of Google Earth imagery.

identified using algorithms to ensure proper distribution of sampling amongst the height classes.

Potential camping sites were also identified, taking into consideration the field mission design factors. Three different scenarios were designed employing 3, 4, and 6 camping sites. Based on ease of operations and cost effectiveness, we chose to implement a 3-campsite approach, sampling 14 sites from each camp, for the 2013 field mission. Figure 5.8 shows the location of the 3 camp sites and their associated plots. Plot center locations were output to a Trimble Juno hand-held GPS, which was used to navigate to designated sampling plots in the field.

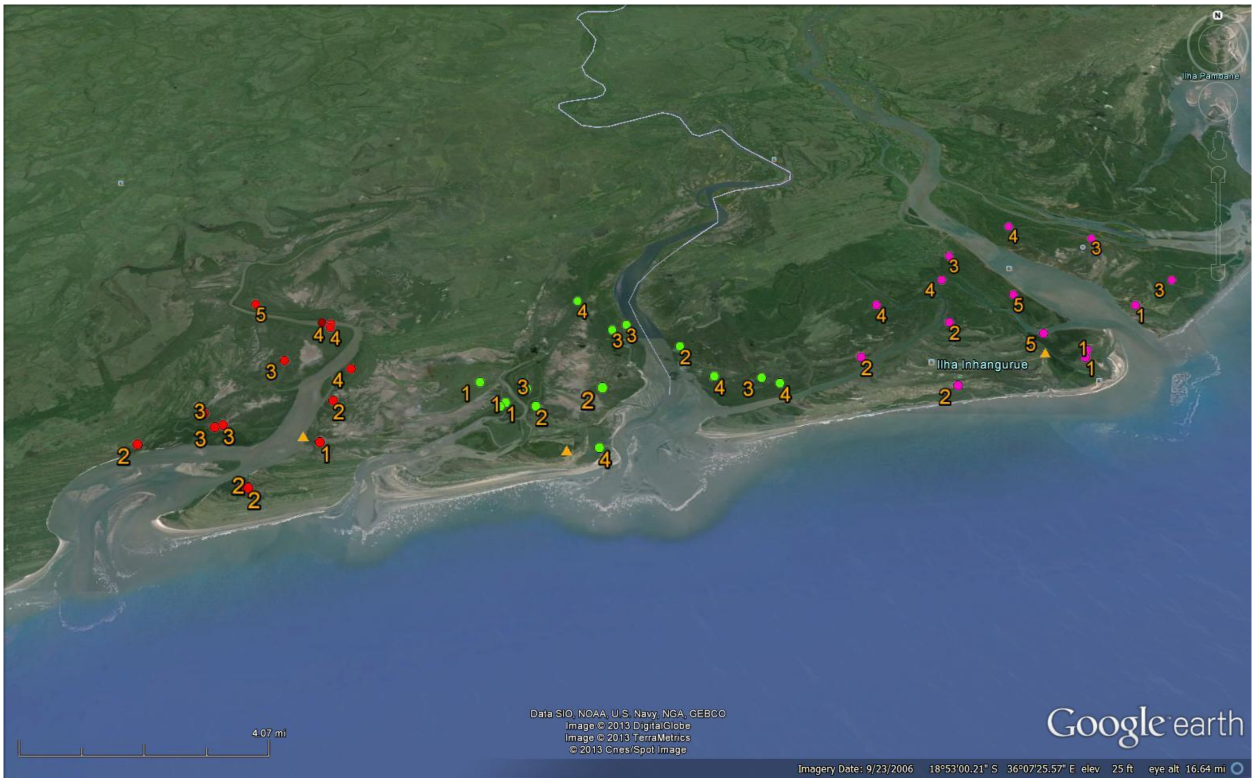

Figure 5.8. Camp and plot locations for the 2013 field mission. Camp sites are the yellow triangles and plot locations are labeled with height canopy classification.

Once in the field, there was a problem accessing the pre-selected plots that were were inaccessible and had to be moved. Accessibility was a major issue with all of the plots associated with the southern camp site (Figure 5.8 red dots). The channel planned for transport was not navigable by boat and reconnaissance attempts to travel in the open ocean proved unsafe with the boats available. We changed our approach accordingly and identified new plot locations within operational range of the second camp, endeavoring to duplicate the same distribution of plots amongst the height classes. Figure 5.9 shows the locations of the actual plots sampled during the field mission. After the field activities, these plots were classified by canopy height class by extracting the mean canopy height from the coverage data set (Figure 5.2) for the coordinates of the plot center.

Figure 5.9. Actual camp (yellow triangles) and plot locations (blue circles) for the 2013 field mission.

5.3 Field Sampling Methods

All field sampling methods were consolidated into a manual that was distributed to field crews for training and reference purposes. The field manual was presented in both English and Portuguese to facilitate training.

5.3.1 Plot Identification and Establishment

The field crew for this mission was large, consisting of 8-10 technical staff and 4-5 support staff. To make daily operations more efficient, plots were identified in advance. This advance team used the GPS and compass to locate and clearly mark the plot center, as well as flag a direct path back to the boat launch. The boat launch location was also vividly marked to help make navigation easier for the boat drivers.

When the crew arrived onsite at the center of the center subplot, the crew leader set about identifying the centers of the other 4 subplots by measuring 29 m in each cardinal direction using a measuring tape. These initial layouts of the tape were also used to identify the four wood debris transects for the center plot.

5.3.2 Height and Diameter Measurements

DBH, height, and species were recorded for both the understory and overstory trees in each subplot. Overstory trees, defined as having a DBH >5 cm, were measured within the 7 m radius circular subplots. All small understory trees and saplings reaching 1.3 m (breast height) were measured within the nested 2 m radius circular subplot within the 7 m radius plot. Large trees, those with a DBH >50 cm, were measured and identified within the 0.5 ha rectangular plot in 2012 and the 0.52 ha square plot in 2013. All diameters were measured to the nearest 0.1 cm using a diameter tape. If the tree was dead, the decay class was recorded in addition to the DBH (Figure 5.10). Some mangroves have root adaptations that affect the way in which diameter is measured; if a buttress stem was encountered, the diameter was measured at the point directly above the buttress. If a tree had prop roots (e.g., *R. Mucronata*), measurements were made just above the highest prop root. In 2013, height was measured (± 0.5 m) for every tree using a Haglof Vertex III hypsometer (Haglof Inc, Sweden). Both diameter and height measurements were subject to quality assurance protocols by the field crew supervisor who repeated these measurements for 5 trees within each subplot. If there was a discrepancy between the 2 measurements greater than 0.3 cm for DBH or 1.0 m for height, then all of the overstory trees in that subplot were re-measured.

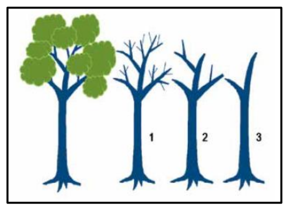

Figure 5.10. Decay classes used to categorize standing dead trees (Kauffman and Donato 2012).

5.3.3 Wood Debris

Wood debris is dead wood laying on the soil surface; it was measured using the planar intersect technique, which involves counting the number of intersections of debris pieces along a transect (Van Wagner 1968,Brown 1971). Four transects, 12 m in length, were established in each subplot (Figure 5.6).   Downed, dead, wood material is classified into four size classes; fine, small, medium, and large (Table 5.2). An aluminum gauge (go-no-go gauge) was used to classify each piece of wood encountered on the transects into size classes. In each of the three smaller size classes, the number of transect intersections is tallied along a designated length of the transect (Table 5.2). The individual diameter was measured for each large wood piece (> 7.6 cm) along the full length of the transect.

Table 5.2. Wood debris size classes and associated diameter range (Brown 1971). The measurement approach column describes how, and for which portion of the transect, each class was measured.

Class	Diameter Range (cm)	Measurement Approach
Fine	0-0.6	Tallied from 10 m to 12 m along transect
Small	0.6-2.5	Tallied from 7 m to 10 m along transect
Medium	2.5-7.6	Tallied from 2 m to 7 m along transect
Large	>7.6	Diameters measured individually along entire transect length

5.3.4 Litter and Ground Vegetation

Two 50 cm x 50 cm microplots were established at the 6 m and 12 m points of each of the 4 subplot transects to collect all litter, except wood debris, down to the mineral soil surface. These 8 samples were composited for each subplot and then weighed in the field to the nearest gram. A subsample of this composite was reserved and transported back to the lab for analysis.

Two 50 cm x 50 cm microplots were established at the 10 m transect point of each of the 4 subplot transects to harvest all ground vegetation < 1.3 m in height. Ground vegetation included any sort of seed, seedling, propagule, or pneumatophore present in the microplot. These 8 samples were composited for each subplot and then weighed in the field to the nearest gram. A subsample of this composite was reserved and transported back to the lab for analysis.

5.3.5 Soils

The soil was sampled to a depth of 200 cm from a point near the center of each subplot using a 1 m gouge auger (AMS Inc, American Falls, Idaho, USA). Soils were sampled at 6 depths (Table 5.3). At each sampling interval, a 5 cm section of the core was cut and extracted. The length of the sample was measured to the nearest mm and the sample placed in a pre-labeled container. The sample interval was adjusted within the layer if the designated zone was disturbed.

Table 5.3. Soil layers represented by samples and the sampling intervals for each soil core.

Sample	Soil Layer (cm below surface)	Sample Interval (cm below surface)
1	0-15	5-10
2	15-30	20-25
3	30-45	35-40
4	45-110	70-75
5	110-185	145-150
6	185-200	190-195

5.4 Laboratory and Data Analyses

The sample preparation, analytical processes and data processing are summarized below, organized by stock components relating to the vegetation biomass and carbon density (Section 5.4.1) and then the soil carbon (Section 5.4.2). The final sections describe how the final total is calculated and the procedures used for descriptive statistics.

5.4.1 Vegetation

The vegetation component includes all analyses associated with live trees, standing dead trees, wood debris, litter, and ground vegetation.

5.4.1.1 Live Trees

The above-ground and below-ground biomass were determined for each tree, both overstory and understory, using published allometric equations for which DBH and wood density are the input parameters. While it is desirable to use species-specific equations developed from regional empirical data (Kaufmann and Donato 2012), unfortunately, equations for East African mangroves don't exist at present, and development of such relationships was outside the scope of this study. Additionally, regional wood density values are not well-documented. As such, we opted to use general equations developed by Komiyama, et al. (2005, 2008) to determine both above-ground (Equation 1) and below-ground biomass (Equation 2):

$$\boldsymbol{B_{AG} = 0.251\rho D^{2.46}} \quad \text{Equation 1}$$

$$\boldsymbol{B_{BG} = 0.199\rho^{0.899} D^{2.22}} \quad \text{Equation 2}$$

Where: B_{AG} and B_{BG} represent above-ground and below-ground biomass (kg), respectively; ρ represents wood density (g cm^{-3}) and D represents DBH (cm).

Komiyama's general equations were selected because they are commonly used throughout the world and are valid for the range of tree diameters measured in the study. Furthermore, the

2011 pilot study associated with this project used these equations and by taking the same approach, we are facilitating an easier comparison of the results among the studies.

The pilot study associated with this project reported wood densities specific to the Zambezi (Bosire, et al. 2012). However, these results had a bias toward high values and were based on a small sample set (Table 5.4)[2]. We wanted to be conservative in our estimates and thereby chose to utilize the mid-value of the density ranges for each species, as published by the World Agroforestry Center (Table 5.4) (2013). The value range published in their database encompasses the other published density values from around the globe that we noted in our literature search. For any tree encountered where the species was unknown, we used the average mid wood density value of the other species, 0.86 g cm^{-3}.

The calculated individual tree biomass values were summed at the subplot level and normalized for the subplot area to provide a total subplot biomass (Mg ha^{-1}). Biomass estimates were converted to carbon using the published carbon concentrations of 0.50 and 0.39 for above-ground and below-ground biomass, respectively (Kauffman and Donato 2012).

Table 5.4. Wood density ranges for each species observed in the Zambezi River Delta (World AgroforestryCenter 2013) and density values reported in the pilot study (Bosire, et al. 2012). The mid value represents the parameter used for determining tree biomass.

Species	Wood Density (g cm^{-3})			
	World Agroforestry Center			Bosire, et al. 2012
	Low	Mid	High	
C. tagal	0.87	0.97	1.09	1.1
B. gymnorrhiza	0.63	0.84	1.05	1.3
X. granatum	0.59	0.70	0.83	0.8
S. alba	0.62	0.78	1.00	0.8
A. marina	0.79	0.81	0.85	0.9
R. mucronata	0.94	1.02	1.12	1.1
H. littoralis	0.83	0.98	1.23	0.8
L. racemosa	0.75	0.88	0.97	-

5.4.1.2 Standing Dead Trees

The above-ground and below-ground biomass for standing dead trees was determined in different ways, dependent on decay class (Figure 5.10). For the above-ground biomass for decay classes 1 and 2, the same general allometric equation was applied for each tree, using a density of 0.69 g cm^{-3}, as species and wood density were not recorded for dead trees, and it has been considered a reasonable estimate of large solid downed wood (Kauffman and Donato 2012). These estimates were adjusted for the loss of leaves and branches by

[2] The 2011 pilot study also reported mangrove biomass and carbon pools. Those findings aren't included or discussed due to differences in approaches, hence inherent incongruities in the basis for reporting.

subtracting 2.5% and 15% of the biomass for classes 1 and 2, respectively (Kauffman and Donato 2012).

The above-ground biomass for class 3 standing dead trees was determined by applying the formula of the volume of a cone:

$$\boldsymbol{V = \pi r^2 \frac{h}{3}} \quad \text{Equation 3}$$

Where: *V* is volume (m^3), *r* is DBH (m) and *h* is the tree height (m).

For those standing dead trees where height was not measured, we estimated the height by applying the equation describing the relationship between DBH and height for all other standing dead trees. Once volume was determined, the value was multiplied by wood density (0.69 g cm^{-3}) to determine biomass.

The below-ground biomass for all classes of standing dead trees was determined by the same general equation used for the live trees, using the standard density value of 0.69 g cm^{-3}. Consideration was made for the swift loss of fine roots once a tree dies. It has been reported that the below-ground biomass of mangroves is composed of a large proportion of fine roots, as much as 66% for some species (Komiyama et al., 1987). We corrected our estimates by subtracting 46%, a conservative estimate still within the ranges reported by other studies (Komiyama, et al. 2000,Komiyama, et al. 1987).

The calculated individual standing dead tree biomass values were summed at the subplot level and normalized for the subplot area to provide a total subplot biomass (Mg ha^{-1}). Biomass estimates were converted to carbon mass by using concentration factors of 0.50 and 0.39 for above-ground and below-ground estimates, respectively (Kauffman and Donato 2012).

5.4.1.3 Wood Debris

Wood debris estimates were determined by first determining the volume of each size class through the use of the following scaling equations (van Wagner 1968, Brown 1971);

$$\boldsymbol{Volume\ (m^2 ha^{-1}) = \pi^2 \left(\frac{ND}{8L}\right)} \quad \text{Equation 4}$$

$$\boldsymbol{Volume\ (m^2 ha^{-1}) = \pi^2 \left(\frac{d_1^2 + d_2^2 + \cdots d_n^2}{8L}\right)} \quad \text{Equation 5}$$

Where: in Equation 4, *N* is the tally count of debris pieces for a given size class, *D* is the mean diameter of that size class (cm), *L* is the transect length (m) and, in Equation 5, *d* is the diameter of each piece of large dead wood.

Equation 4 is used for the medium, small, and fine classes and Equation 5 is used only for the large size class. We used the mean diameter of the standard range for each of the 3 smaller size classes (Table 5.5). The volume of each size class was converted to biomass by multiplying by wood density (Table 5.5). We did not collect samples to determine wood densities specific to the Zambezi, so we used density values reported by Kauffman and Donato

(2012). The biomass estimates were converted to carbon mass by using a concentration of 0.50, as recommended by Kauffman and Donato (2012).

Table 5.5. Diameter and density values used to determine wood debris volume and mass.

Size Class	Diameter (cm)	Density (g cm^{-3})
Large	as measured	Solid- 0.69 Decayed- 0.29
Medium	5.25	0.71
Small	1.55	0.64
Fine	0.30	0.48

5.4.1.4 Litter and Ground Vegetation Biomass

The litter representative subsamples from each plot were returned to the lab[3] to determine the moisture content. The wet samples were weighed in the lab and then placed in a 60°C drying oven and dried until a constant weight was achieved. After cooling, the dry sample was reweighed and the ratio between the wet and dry mass determined. This ratio was then used to adjust the mass of the whole litter sample to a dry-weight basis, which was then scaled to a per-hectare estimate. Mass was converted to carbon concentration by applying a recommended conversion factor of 0.45, representative of the mean carbon concentration of tropical forest litter (Kauffman and Donato 2012). Ground vegetation biomass measurements were scaled to a per-hectare estimate and converted to carbon mass by applying the same conversion factor of 0.45, as recommended by Kauffman and Donato (2012).

5.4.2 Soils

Soil samples were returned to the lab[4] for the determination of the air-dried weight of the volumetric sample. Soils were placed in a 60°C oven and dried until a constant weight was achieved. A 50 member subset of samples was used to determine the oven-dried weight. A subsample was weighed and placed in a 105°C oven and dried until a constant weight was achieved. The air-dried to oven-dried ratio was calculated for each of these samples and the average (1.010 ± 0.003) applied to the air-dried mass of all soil samples to adjust the mass to an oven-dried basis. The bulk density (g cm^{-3}) of each sample was calculated by dividing the oven-dried mass by the volume of the sample. Prior to further analysis, a subset of 100 soil samples was tested for the presence of carbonates following standard procedures (Thomas 1996)

[3] Samples were processed at the Biology Department, Univsidade Eduardo Mondlane, Maputo.
[4] Same as Footnote 3.

The carbon concentration of each soil sample was determined on pulverized subsamples using a Perkin Elmer 2400 Series II CHNS/O Analyzer (Perkin Elmer, Waltham, MA, USA)[5]. Instrument settings and procedures followed the recommended application protocols described by Perkin Elmer (2010). Quality assurance of analyses was provided by the analysis of duplicates, and calibration of the instrument with certified standards. The precision of duplicate samples was ± 0.1% C or better.

Soil sample carbon density was determined as follows:

$$\boldsymbol{C_S^n} = \boldsymbol{D_b} * \boldsymbol{d} * \boldsymbol{C} \quad \text{Equation 6}$$

Where: C_S^n is the soil carbon concentration (Mg ha^{-1}) for interval n (n =1, 2,…,6), D_b is the bulk density (g cm^{3}), d is the depth interval (cm), and C is the sample carbon concentration, expressed as a percent.

The carbon density of each layer within a core was summed to determine the total soil carbon density for that subplot.

5.4.3 Ecosystem Carbon Stock

The ecosystem carbon density (Mg ha^{-1}) for each height class was estimated by summing the carbon density values for each of the component pools[6]. The equation for the ecosystem carbon stock is:

$$\boldsymbol{Ecosystem\ C} = \boldsymbol{C_{O-AGB}} + \boldsymbol{C_{O-BGB}} + \boldsymbol{C_{U-AGB}} + \boldsymbol{C_{U-BGB}} + \boldsymbol{C_{D-AGB}} + \boldsymbol{C_{D-BGB}} + \boldsymbol{C_L} + \boldsymbol{C_{GV}} + \boldsymbol{C_{WD}} + \boldsymbol{C_S} \quad \text{Equation 7}$$

Where: each term is the carbon concentration (Mg ha^{-1}) for each component, as follows: $C_{O\text{-}AGB}$ and $C_{O\text{-}BGB}$ are overstory above-ground and below-ground biomass, respectively; $C_{U\text{-}AGB}$ and $C_{U\text{-}BGB}$ are understory above-ground and below-ground biomass, respectively; $C_{D\text{-}AGB}$ and $C_{D\text{-}BGB}$ are standing dead tree above-ground and below-ground biomass, respectively; C_L is litter; C_{GV} is ground vegetation; C_{WD} is wood debris; and C_S is soils.

Once a per-hectare estimate was obtained for each height class, the ecosystem carbon stock was estimated by multiplying each of the height class total carbon densities by their respective areas (Table 5.6) and summing them together to arrive a final carbon mass (Mg).

[5] Analyses conducted at either the Center for Forested Wetland Research, Southern Research Station, US. Forest Service, Cordesville, South Carolina, U.S.A. or the University of Georgia, Odum School of Ecology Analytical Laboratory, Athens, Georgia, U.S.A.

[6] Carbon density can be converted to carbon dioxide equivalents (CO_2e) by multiplying by 3.67.

Table 5.6. Area for each canopy height class within the Zambezi River Delta.

Canopy Height Class	Area (ha)
1	4,730
2	10,536
3	8,610
4	5,522
5	869
Total Mangrove Area	**30,267**

5.4.4 Statistics

Sample means, along with variances and 95% confidence intervals, were computed for each stratum based on the two-stage sampling design using SAS Statistical Software - PRC SURVEYMEANS (SAS Inc.) without the finite population correction because the sampling fraction was very low.

Individual strata totals were obtained by multiplying each stratum mean by its area (N_h , h=1,2,3,4,5) and the variance computed as N_h^2 times the variance of its stratum mean. Overall means and variances combined over all strata were computed as:

$$\bar{X} = \sum_{h=1}^{5} W_h \bar{X}_h \quad \text{Equation 8}$$

Where: $W_h = N_h / N$ and $N = N_1 + N_2 + N_3 + N_4 + N_5$, with variance:

$$Var\left(\bar{X}\right) = \sum_{h=1}^{5} W_h^2 Var\left(\bar{X}_h\right) \quad \text{Equation 9}$$

Overall uncertainties surrounding the totals were then $TOTAL = N\bar{X}$ with variance:

$$Var\left(TOTAL\right) = N^2 Var\left(\bar{X}\right) \quad \text{Equation 10}$$

6 Results

6.1 Forest Composition and Structure

Eight mangrove species were identified in the overstory and understory: *A. marina, B. gymnorrhiza*, *C. tagal*, *R. mucronata*, *S. alba*, *H. littoralis*, *L. racemosa*, and *X. granatum*. Overstory trees that could not be identified were included in an “unknown” category for descriptive and analytical purposes.

Figure 6.1. Dense *C. tagal* stand in the Zambezi River Delta.

C. tagal was the most frequently observed species in the overstory (Fig. 6.1), accounting for 25.5% of all trees, second in abundance was *R. mucronata* (18.4%). *L. racemosa* was the rarest of the overstory trees, contributing only 0.5% of the total trees measured. Unknown trees accounted for 1.7% of the overstory. The understory was also dominated by *C. tagal*, accounting for 53.4% of the trees. *B. gymnorrhiza*, was second-most frequent understory tree comprising 9.5% of the total. The least observed understory species were *S. alba* and *L. racemosa*, representing 0.6% and 0.3% of the total, respectively. The overstory species composition varied widely among strata (Figure 6.2A), with at least 7 of the 8 mangrove species observed in each height class. Unknown overstory species were present in each height class. Understory trees were absent from 15% of the plots sampled. The lack of saplings was most pronounced in height classes 4 and 5, in which there was no understory trees observed in 30% and 29% of the plots sampled, respectively. The understory species composition (Figure 6.2B) was the most varied in height classes 1 and 4, with 7 mangrove species recorded. The understory trees in height class 5 were composed of 4 species, but dominated by *B. gymnorrhiza* and *H. littoralis.*

The structural attributes of the overstory mangroves varied by height class (Table 6.1), with mean heights ranging from 7.0 m to 12.9 m in height classes 1 and 5, respectively. Mean tree diameter also increased with height class, ranging from 8.8 cm to 14.3 cm in height classes 1 and 5, respectively. Basal area mean values ranged from 13.7 m^2 ha^{-1} to 40.8 m^2 ha^{-1}. The understory stand characteristics exhibited a smaller range in variability (Table 6.1). Mean tree height was greatest in height class 2, at 4.1 m, and the smallest in height class 5, at 2.2 m. The understory mean tree diameter ranged from 2.3 cm to 3.1 cm and basal area means ranged from 1.2 m^2 ha^{-1} to 4.0 m^2 ha^{-1}.

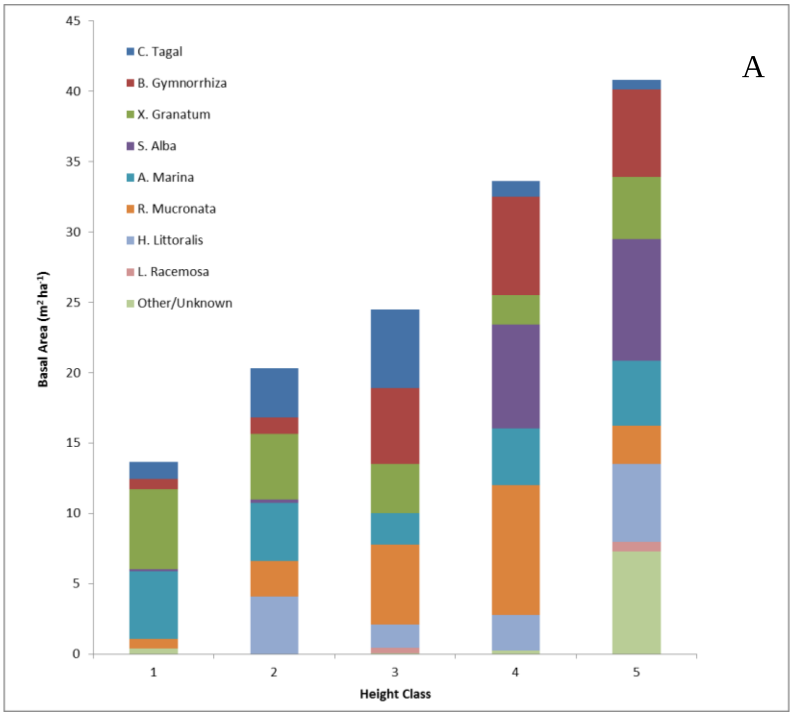

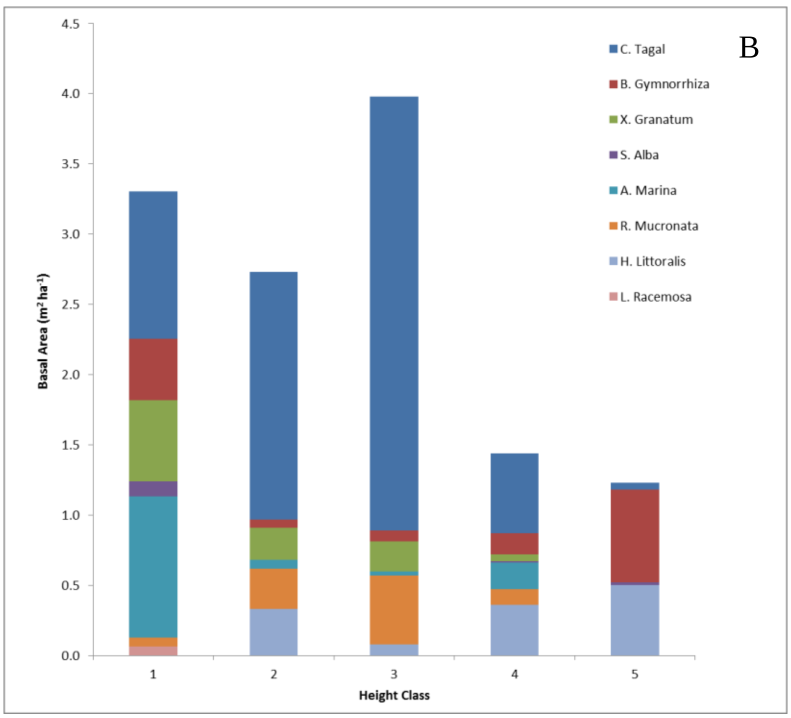

Figure 6.2. Basal area proportioned by species and height class for the (A) overstory and (B) understory trees.

Table 6.1. Stand characteristics (mean and standard error) for overstory and understory trees, summarized by height class.

Metric	Height Class									
	1		2		3		4		5	
	Mean	**S.E.**	**Mean**	**S.E.**	**Mean**	**S.E.**	**Mean**	**S.E.**	**Mean**	**S.E.**
Overstory										
Height (m)	7.0	0.4	7.9	0.6	10.4	0.6	12.1	0.7	12.9	1.0
Diameter (cm)	8.8	0.5	9.7	0.5	10.4	1.1	12.8	0.6	14.4	1.0
Basal Area (m^2 ha^{-1})	13.7	2.8	20.3	2.8	24.5	3.1	33.6	3.2	40.8	4.7
Tree Density (stems ha^{-1})	1853.0	305.4	2199.4	200.5	2234.6	332.0	2045.5	134.7	1848.5	185.9
Understory										
Height (m)	3.2	0.6	4.1	0.3	3.9	0.4	3.1	0.1	2.2	0.1
Diameter (cm)	2.4	0.1	3.0	0.1	3.1	0.2	2.9	0.2	2.3	0.4
Basal Area (m^2 ha^{-1})	3.3	1.6	2.7	0.8	4.0	2.0	1.4	0.5	1.2	0.6
Tree Density (stems ha^{-1})	6000.0	3030.5	3491.8	866.3	4914.3	2268.1	1808.0	722.3	2346.7	1564.0

6.2 Carbon Stocks: Biomass

The above-ground contribution to the total ecosystem carbon stock consists of 6 sub-components: overstory, understory, ground vegetation, woody debris, litter, and standing dead trees. The overstory carbon density ranged from 14.8 Mg ha^{-1} to 445.9 Mg ha^{-1} (Table 6.2). The understory tree carbon density reflects the variation in stocking of the smaller trees, ranging from 0 to 108.17 Mg ha^{-1} (Table 6.2).

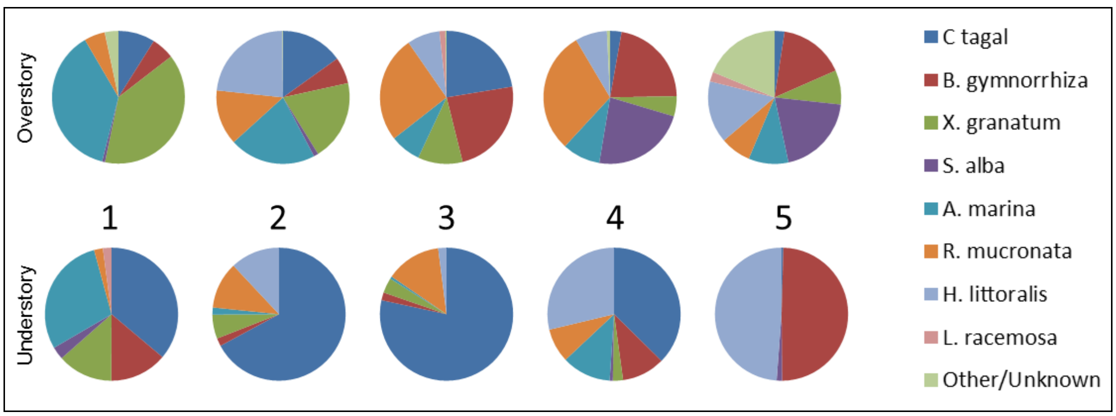

Figure 6.3. Proportional contribution of each species to above-ground biomass carbon density for overstory trees (top) and understory trees (bottom).

The above-ground biomass contribution to biomass carbon density at the species level varied by height class for both overstory and understory trees (Figure 6.3) and was analogous to the species-proportioned basal area values for each height class (Figure 6.2). In general, the species distribution among height classes was heterogeneous. The most pronounced dominance exhibited in the overstory occurred in height class 1, where *X. granatum* and *A. marina* contributed 39% and 38%, respectively, to the total carbon density. *C. tagal* is the principal contributor amongst the understory trees, constituting as much as 78% of the total in height class 3, which had the largest understory above-ground biomass carbon density. *L. racemosa* consistently contributed the least amount of carbon, with overstory contributions ranging from 0 in height classes 2 and 4, to only 2% in height class 5 and only one understory contribution, in height class1, of 0.4%.

The ground vegetation sub-component contributes a small proportion of carbon to the overall ecosystem stock (Table 6.2), with height class means ranging from a few kilograms to 0.17 Mg ha^{-1}. There were plots in each height class that didn't have ground vegetation. Height classes 1 and 5 had 33% and 29% of plots exhibiting an absence of understory biomass, respectively. However, in both classes 2 and 3, only 13% and 15% of plots, respectively, had contributions from this component and class 4 had 30% of plots with understory biomass present. It is important to note that this component does not include contributions from the mangrove fern, *A. aureum*. The fern was present in several plots; unfortunately, the established protocol did not include provisions for the large ferns[7]. However, while in the field, we attempted to measure the biomass by expanding the size of the microplot, the resulting estimates ranged from 25 to 68 Mg ha^{-1}.

The carbon density of wood debris values ranged from 0.4 to 24.8 Mg ha^{-1} and means ranged from 6.7 Mg ha^{-1} for height class 1 to 12.5 Mg ha^{-1} for class 5 (Table 6.2). Woody debris was observed in all of the plots sampled. The litter carbon density values ranged from 0 to 6.0 Mg ha^{-1} and height class means ranged from 0.2 Mg ha^{-1} for class 1, to 0.7 Mg ha^{-1} for class 5 (Table 6.2). Nineteen percent of all plots sampled had no litter present. Litter contributions to the carbon pool were low, with 46% of plots containing less than 1 Mg C ha^{-1}.

Figure 6.4. Measuring tree diameter in an *R. mucronata* stand.

Standing dead tree carbon density ranged from 0 to 39.9 Mg ha^{-1}, with height class means ranging from 3.7 Mg $ha^{-1}$for class 2, to 10.9 Mg ha^{-1} for class 5 (Table 6.2). Only 4% of sampled plots lacked standing dead trees. Standing dead trees accounted for 8% of all overstory trees.

[7] As result of this experience the field sampling protocol will be modified to include provisions to ensure that the tree-fern biomass is adequately represented in the biomass inventory.

The above-ground carbon pool is dominated by the overstory (Figure 6.6), accounting for 73% of the total biomass pool in height class 1, 83% in height classes 2 and 3, and 89% in classes 4 and 5. The ground vegetation and litter were the smallest components, with each contributing 0.2% or less to the total carbon pool. The remaining three sub-components (understory trees, standing dead trees, and wood debris) contribute amounts ranging from 1-10% of the total above-ground vegetation pool.

Figure 6.5. Tallying wood debris along a transect.

Table 6.2. Carbon density (mean and standard error) in above-ground (AGB) and below-ground biomass (BGB) components for each height class.

	Carbon Density (Mg ha^{-1})									
	1		2		3		4		5	
	Mean	**S.E.**	**Mean**	**S.E.**	**Mean**	**S.E.**	**Mean**	**S.E.**	**Mean**	**S.E.**
Above-Ground Biomass										
Overstory	55.36	11.78	96.66	16.45	127.36	20.17	183.34	20.61	241.31	36.24
Understory	7.65	3.69	7.44	2.28	11.05	5.67	3.74	1.28	2.98	1.40
Ground Vegetation	0.12	0.11	0.01	0.01	0.14	0.08	0.17	0.16	0.05	0.02
Woody Debris	6.72	3.77	7.77	1.20	6.78	1.06	9.23	1.87	12.51	3.75
Litter	0.17	0.07	0.29	0.19	0.31	0.16	0.37	0.14	0.66	0.20
Standing Dead Tree	5.37	3.70	3.70	1.00	6.89	1.34	9.20	3.08	10.97	4.93
Total AGB	**75.39**	**12.58**	**115.86**	**16.80**	**152.54**	**17.72**	**206.05**	**20.49**	**268.47**	**36.56**
Below-Ground Biomass										
Overstory	18.94	3.83	31.72	5.01	40.36	5.88	56.28	5.55	69.68	9.43
Understory	3.63	1.75	3.41	1.02	5.03	2.56	1.70	0.59	1.39	0.66
Dead Standing Tree	1.27	0.87	0.87	0.24	1.51	0.27	1.71	0.47	1.71	0.76
Total BGB	**23.84**	**3.10**	**36.00**	**5.02**	**46.90**	**5.05**	**59.70**	**5.18**	**72.77**	**9.42**

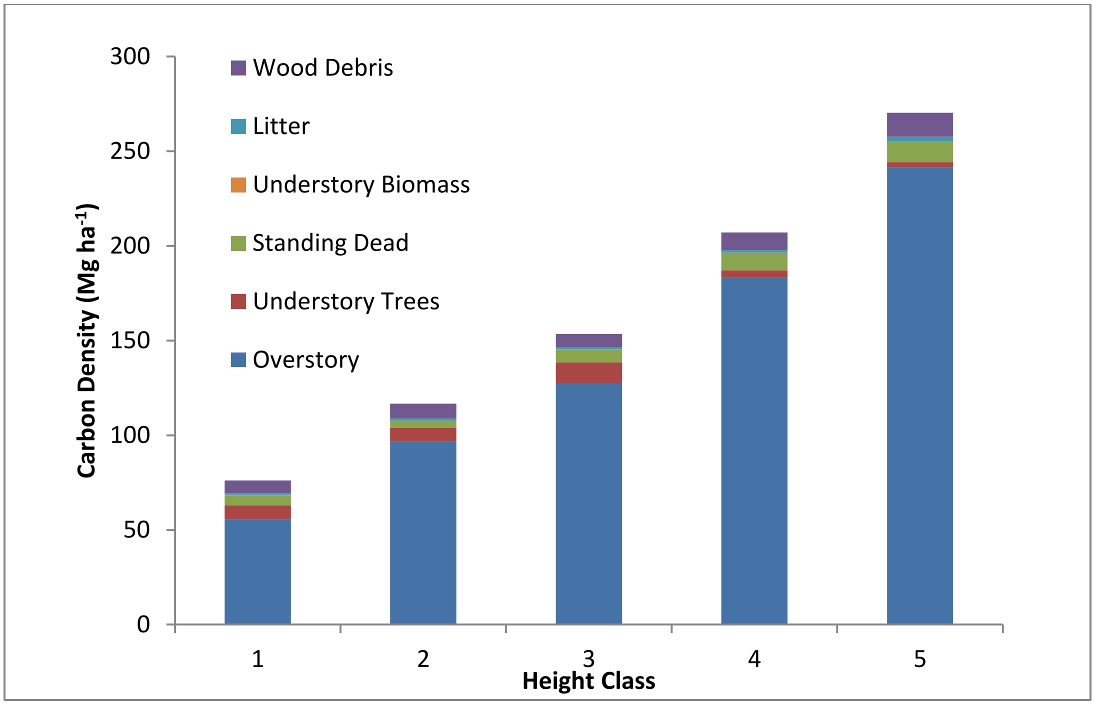

Figure 6.6. Contributions of biomass components to above-ground carbon density; the values represent the average within height classes.

Below-ground biomass comprises overstory, understory, and standing dead tree components (e.g., roots). The overstory below-ground biomass carbon density ranged from 5.7 to 71.2 Mg ha^{-1}. Height class mean density values increase with each subsequent class, ranging from 18.9 to 69.7 Mg ha^{-1} (Table 6.2). The ratio of overstory AGB to BGB ranged from 0.34 for height class 1 to 0.29 for height class 5. The understory below-ground biomass carbon density height class means ranged from 1.4 Mg ha^{-1} for height class 5, to 5.0 Mg ha^{-1} for height class 3 (Table 6.2). The standing dead tree below-ground biomass carbon density height class means ranged from 0.9 Mg ha-1 for height class 2, to 1.7 Mg ha-1 for both height classes 4 and 5.

The overstory BGB is the dominant component in all five height classes, comprising from 79% of the total pool in height class 1, to 96% of the total in height class 5 (Figure 6.7). The understory sub-component was largest in height class 1, at 15% of the total, and least significant in height classes 4 and 5, comprising 3% and 2% of the total, respectively. The contribution of the standing dead tree sub-component to the total pool was the most consistent amongst the height classes, comprising 5% of the total BGB in height class 1 and 2%-3% of the pool in the remaining 4 height classes.

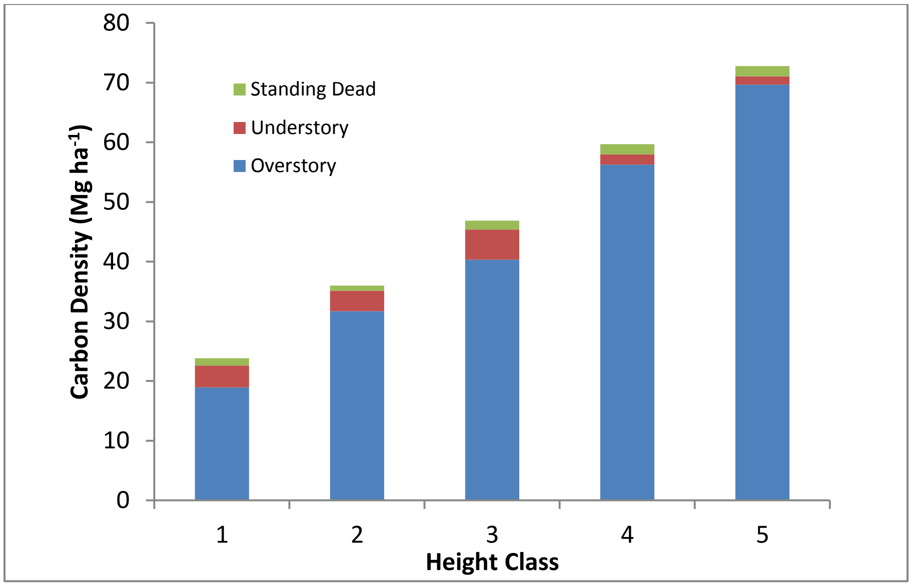

Figure 6.7. Contribution of biomass components to below-ground carbon density; the values represent the average within height classes.

6.3 Carbon Stocks: Soils

The mean soil bulk density ranged from 0.80 to 0.85 g cm^{-3}, exhibiting a generally increasing trend with depth (Figure 6.8A; Table 6.3). The mean carbon concentration decreased with depth, with the exception of interval 2; interval 1 had a mean of 2.09%, decreasing to 1.57% at interval 6 (Figure 6.8B; Table 6.3). The soil carbon density to a depth of 200 cm ranged from 274.6 Mg ha^{-1} for class 1, to 314.1 Mg ha^{-1} for class 3 (Table 6.4).

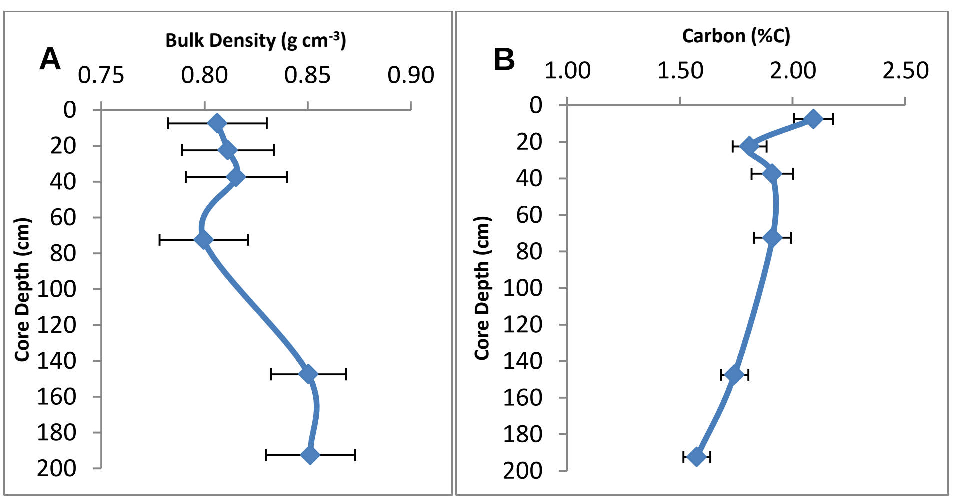

Figure 6.8. Mean soil bulk density (A) and carbon concentration (B) with depth; error bars represent the standard error.

Table 6.3. Soil bulk density, carbon concentration, and carbon density means and standard errors for each layer within height classes.

		Bulk Density ($g\ cm^{-3}$)		%C		Carbon Density ($Mg\ ha^{-1}$)	
Height Class	**Soil Depth (cm)**	**Mean**	**S.E.**	**Mean**	**S.E.**	**Mean**	**S.E.**
1	0-15	0.94	0.06	1.74	0.18	23.44	1.47
	15-30	0.93	0.06	1.59	0.15	21.49	1.14
	30-45	0.95	0.05	1.53	0.11	21.07	1.79
	45-110	0.92	0.08	1.49	0.22	83.53	7.70
	110-185	0.85	0.03	1.73	0.20	110.00	12.33
	185-200	0.84	0.02	1.56	0.11	19.23	1.34
2	0-15	0.81	0.04	2.01	0.14	23.40	1.27
	15-30	0.84	0.04	1.69	0.11	20.24	0.86
	30-45	0.83	0.05	1.81	0.16	20.71	0.95
	45-110	0.80	0.04	1.93	0.17	94.59	5.72
	110-185	0.88	0.04	1.69	0.09	108.02	4.31
	185-200	0.90	0.04	1.45	0.08	18.76	0.82
3	0-15	0.77	0.05	2.25	0.18	24.33	1.11
	15-30	0.78	0.04	2.03	0.19	22.16	1.09
	30-45	0.79	0.05	2.11	0.22	22.99	1.36
	45-110	0.78	0.03	2.07	0.12	100.15	3.67
	110-185	0.83	0.03	1.84	0.13	110.07	7.14
	185-200	0.83	0.05	1.73	0.17	20.09	1.55
4	0-15	0.74	0.06	2.28	0.20	24.08	1.11
	15-30	0.71	0.04	1.89	0.14	19.46	0.89
	30-45	0.72	0.05	2.12	0.18	21.67	1.07
	45-110	0.73	0.04	1.99	0.14	90.66	4.58
	110-185	0.81	0.05	1.73	0.10	101.61	4.46
	185-200	0.80	0.05	1.63	0.10	18.92	1.20
5	0-15	0.77	0.05	2.36	0.19	26.66	2.05
	15-30	0.78	0.05	1.94	0.11	22.42	1.45
	30-45	0.81	0.04	1.94	0.15	22.68	1.20
	45-110	0.79	0.04	1.75	0.12	88.58	5.45
	110-185	0.89	0.06	1.63	0.22	101.43	7.21
	185-200	0.92	0.10	1.50	0.32	18.93	2.92

6.4 Ecosystem Carbon Stock

The carbon densities within the three principal pools (above-ground and below-ground vegetation, and soils) were summed to determine an ecosystem-level carbon density (Mg ha^{-1}) for each height class (Table 6.4). The total carbon density, the combination of biomass and soils, ranged from 373.8 Mg ha^{-1} for height class 1, to 620.8 Mg ha^{-1} for height class 5 (Table 6.4). The soil component constitutes the largest proportion of the total carbon density, comprising 45%-73% of the total pool (Figure 6.9).

Table 6.4. Carbon density (mean and standard error) for above- and below-ground biomass and soil pools within each height classes, and the corresponding ecosystem carbon stock.

	Carbon Density (Mg ha^{-1})									
	1		2		3		4		5	
	Mean	**S.E.**	**Mean**	**S.E.**	**Mean**	**S.E.**	**Mean**	**S.E.**	**Mean**	**S.E.**
Total AGB	75.4	12.6	115.9	16.8	152.5	17.7	206.0	20.5	268.5	36.6
Total BGB	23.8	3.1	36.0	5.0	46.9	5.1	59.7	5.2	72.8	9.4
Soils	274.6	25.0	282.2	11.2	314.1	14.8	279.8	13.6	279.6	17.6
Total	**373.8**	**29.5**	**434.1**	**24.5**	**513.5**	**27.1**	**545.5**	**29.0**	**620.8**	**49.0**

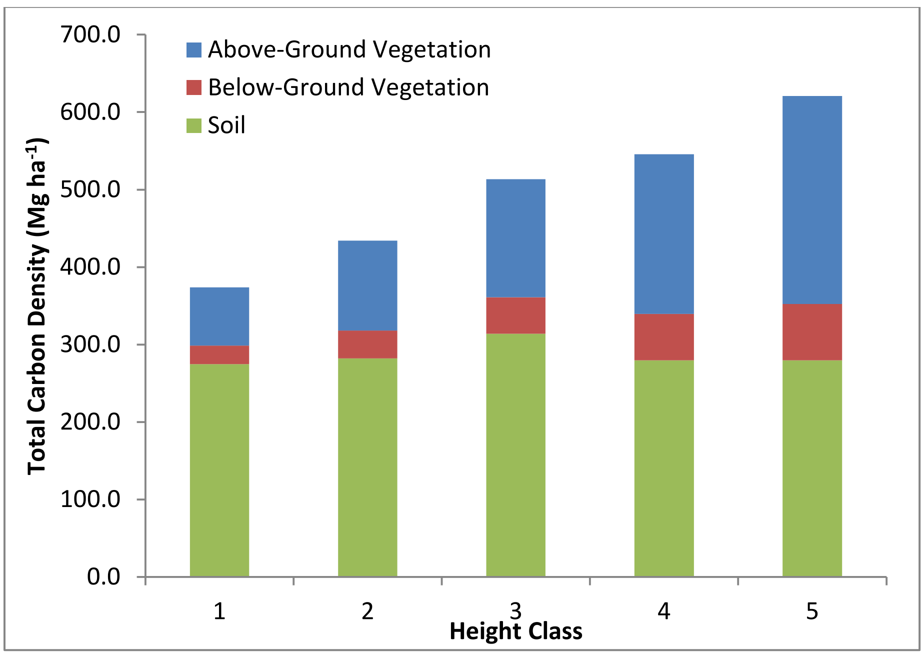

Figure 6.9. Contributions of biomass and soil carbon pools to ecosystem carbon density within height classes. Values represent the mean of each height class.

The soil percentage is greater in the smaller height classes, where the above-ground vegetation is not as large as in the taller height categories (class 4 and 5). The contribution of the below-ground biomass to the ecosystem carbon stock ranges from 6% in class 1 to a high of 12% in class 5.

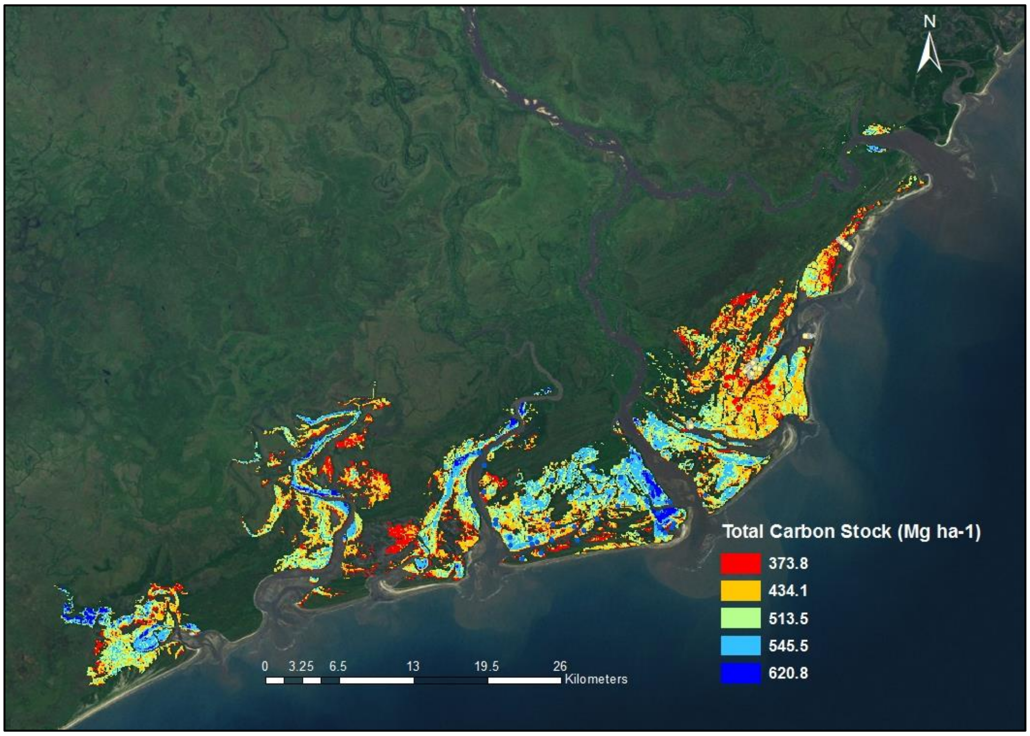

Figure 6.10. Spatial distribution of mangrove ecosystem carbon stocks in the Zambezi River Delta.

The ecosystem carbon stock for the Zambezi River Delta is 1.43 x 10^7 Mg (Std. Err.: 4.1 x 10^5 Mg) carbon (Table 6.5). The spatial distribution of carbon in the mangroves on the Zambezi River Delta is shown in Fig. 6.10.

Table 6.5. Total carbon mass calculated for each height class and total ecosystem carbon stock estimate.

Height Class	Total Carbon Stock (Mg C ha^{-1})	Area (ha)	Total Carbon (Mg * 10^6)
1	373.84	4,730	1.8
2	434.05	10,536	4.6
3	513.51	8,610	4.4
4	545.51	5,522	3.0
5	620.82	869	0.5
	Total	**30,267**	**14.3**

7 Discussion

7.1 Inventory Design and Spatial Decision Support System

While many assessments of mangrove carbon pools have taken a synoptic approach, whereby a relatively few number of sample plots are arbitrarily located within the forest, we used a stratified random sampling design because they have been shown to be more effective and efficient in forest inventories (Cormack 1988,Nusser, et al. 1998). The application of the canopy height as the basis for stratification proved effective. The canopy height classes reflected variations in stand density and height that caused the corresponding differences in biomass and carbon estimates (e.g. Fig 6.9). Most of the mangrove species were represented in each of the height classes, indicating a heterogeneous distribution of species across the Delta. Accordingly, the sampling design appears to have encompassed the range in physical stand conditions as well as composition of the forest.

Mangroves are typically remote and difficult to access, and that is certainly the case with respect to the Zambezi River Delta. The SDSS was developed to provide an unbiased allocation of sample plots while accommodating logistical and operational constraints. The application of the SDSS proved effective in allocating the prescribed number of measurement plots given the imposed constraints. While not all of the established plots corresponded directly with the pre-selected locations, appropriate steps were taken in the field to select viable replacement sites that sustained the integrity of the inventory design. Canopy height class maps were examined onsite to select backup plots that were in the same height class as those that needed to be replaced. Our inability to access the plots in the southern portion of the Delta reflected an incongruity in matching the characteristics of the waterways with the available boats, and thereby effectively excluded a portion of the southern Delta from sampling. However, given the small confidence intervals around the biomass and carbon estimates, we feel that the calculated pools are applicable to the entire inventory area. .

7.2 Forest Composition

There were 8 mangrove species in the overstory and understory trees in the Zambezi River Delta, representing all of the major species reported to be present in Mozambique (Taylor et al., 2003, Beentje and Bandeira 2007): *C. tagal, B. gymnorrhiza, X. granatum, S. alba, A. marina, R. mucronata, H. littoralis,* and *L. racemosa*. Additional species reported to be in Mozambique that were not observed in this study are *P. acidula*, which is found only in northern and southern portions of the country (Barbosa, et al. 2001,Beentje and Bandeira 2007), and *X. moluccensis* (Lam.) M. Roem., which is not recognized with the East Africa eco-region (http://www.iucnredlist.org/details/178805/0), although some have reported it in the Zambezi River Delta (Bosire, et al. 2012). While not located within the sample plots, various palms were observed in the Delta. Additionally, mangrove fern, *A. aureum*, occurred in dense patches throughout the study area.

The species contributing the most to stand density were *R. mucronata*, *B. gymnorrhiza*, *X. granatum*, and *A. marina*. *L. racemosa* was the rarest species and contributed the least to stand basal area. These major species are comparable to the composition of mangrove forests in the northern and southern regions of Mozambique (Barbosa, et al. 2001,Bandeira, et al.

2009). The overstory species were well-distributed amongst the classes (Figure 6.2A), with no clear trends or patterns in occurrence related to canopy height class.

The understory tree density was inversely related to the overstory, with the smaller height classes having the higher amounts. Presumably that relationship reflects lower light availability with the taller stands (Feller and Sitnik 1996). A distinguishing factor with the lower understory density in the height classes 4 and 5 was the fewer number of stems as compared to the other classes. The understory was dominated by *C. tagal*, accounting for over 50% of the stems and understory basal area.

7.3 Carbon Stocks - Biomass

Contributions to the carbon pool from litter and ground vegetation are both insignificant, with both components contributing less than 0.7 Mg C ha^{-1} in each height class. This finding corroborates reports from other studies that suggest the ground vegetation layer is generally negligible (Janzen 1985) and is why it is frequently not sampled (e.g., (Donato, et al. 2012). Woody debris constituted a mean of 6% to the AGB carbon density, a value slightly less than means of other studies, which are generally in the range of 10-15% (Adame, et al. 2013,Kauffman, et al. 2011,Donato, et al. 2012,Kauffman, et al. 2014).

While we are reporting a very small amount of carbon in the ground vegetation layer, it is important to reiterate that we did not include the mangrove fern, *A. aureum,* in our ground vegetation biomass calculations. As such, our ground vegetation carbon density values should be considered an under estimation. Our existing field protocols for sampling ground vegetation were not appropriate for sampling the dense patches of mangrove fern. These experiences will inform future field missions and will be taken into account when we develop a revised version o the sampling protocols[8].

The AGB carbon density for the height classes ranged from 75.4 to 268.5 Mg C ha^{-1}. Most of the studies completed on African mangroves have reported results in terms of biomass, rather than carbon density. To facilitate comparison, we have multiplied published biomass data by 0.5 to convert the reported values to carbon density. Gazi Bay, Kenya, a well-studied mangrove setting, has had a variety of estimates made with regard to the *Rhizopora* AGB. Slim et al. (1996) and Kirui et al. (2006) produced estimates of 125 Mg C ha^{-1} to 226 Mg C ha^{-1}, respectively. More recently, Cohen et al. (2013) provided an estimate of 67 Mg C ha^{-1}. Research on mangroves in French Guiana provided a range of 16 Mg C ha^{-1} to 158 Mg C ha^{-1} (Fromard, et al. 1998). The variances exhibited in estimates at large spatial scales are most likely indicative of differences in forest composition, climatic conditions, hydrology, geomorphology, successional stage and history of disturbances (Fromard, et al. 1998, Cohen, et al. 2013).

The BGB estimates increased linearly (r^2 = 0.96) from 23.7 Mg C ha^{-1} to 72.8 Mg C ha^{-1} with the mean measured tree height in each height class. The ratio of BGB to AGB ranged from 0.29 to 0.34 reflecting the parameterization of the allometric equations, but lower than the ratios (0.6-

---

[8] The field sampling protocols used for this study are being updated and will be provided to WWF-Mozambique and Ministry of Agriculture for subsequent assessments of mangrove carbon stocks.

0.8) reported for other global mangroves (Kauffman and Donato 2012,Komiyama, et al. 2008). While these studies utilized the same BGB allometric equation introduced by Komiyama, et al. (2005), they also used appropriate, regionally-specific allometric equations for AGB, which most likely resulted in the different calculated ratios. Mangrove root biomass characterization suffers from well-known difficulties in field measurements and in developing appropriate allometric equations (Kauffman, et al. 2011). These challenges mean that the difference in ratios exhibited is more likely an artifact of methodologies, rather than reflective of an actual difference in mangrove structure.

The disparity of the Zambezi mangroves' root-to-shoot ratios to those reported in other global studies highlights the need to validate allometric equations for the East Africa region. Since most studies utilize the same BGB allometric equation, any differences in the BGB to AGB ratio will be due to differences in the allometric equation chosen for above-ground biomass determination. Validating equations for the region will inform better allometric equation choices and ultimately result in more reliable biomass estimations.

While tree height measurements were obtained during this field mission, they will only be used in this case for validating remote-sensing data sets. This is only one potential use of these data, as the collection also provides added flexibility when selecting allometric equations, some of which are dependent on tree height as an input parameter. Tree height measurement can be a time-consuming process, as it can difficult to distinguish individual tree crowns in the canopy; accordingly, the importance and potential utilization of these values should be weighed against the time commitment required to obtain them.

7.4 Carbon Stocks - Soil

Our soil carbon concentration means for each sampling depth, ranging from 1.5% to 2.4% (Table 6.3), are similar to those reported in a recent compilation of global mangrove sediment data, which cited a median carbon concentration of 2.2% (Kristensen, et al. 2008). The same review illustrated that 44% of the available literature data shows carbon less than 2% and 28% has values between 2 and 5% (Kristensen, et al. 2008), suggesting that the carbon concentrations in the Zambezi are in the same range as 72% of the published data.

Our calculated soil carbon pool (275 Mg ha^{-1} to 314 Mg ha^{-1}) is lower than what has been reported in several recent mangrove ecosystem carbon stock studies (Kauffman, et al. 2011,Donato, et al. 2012,Kauffman, et al. 2014,Wang, et al. 2013). The principal factors affecting the determination of soil carbon stocks are bulk density, C concentration, and the total depth over which the estimates are integrated. Others studies focused on quantifying ecosystem carbon stocks typically report mangrove bulk density values in the range of 0.2 g cm^{-3} to 0.6 g cm^{-3} and carbon concentrations of 9% to 26% (Kauffman, et al. 2011,Donato, et al. 2012,Kauffman, et al. 2014,Wang, et al. 2013). Only a recent carbon stock study in Madagascar (Jones, et al. 2014) reported soil characteristics that were similar to that observed in the Zambezi River Delta, with bulk density values ranging from 0.52 g cm^{-3} to 1.39 g cm^{-3} and carbon concentrations ranging from 0.6% to 6.1%.

Differences in sampling approaches, specifically with regard to core sampling depth, make inter-comparison of study results difficult. Because carbon stocks are commonly reported on a per-area basis, one can't immediately discern the basis of reporting by the value alone. Donato, et al. (2012) report soil carbon pools ranging from 517 Mg ha^{-1} to 947 Mg ha^{-1}, but they integrated sample analyses over a depth of 3 m, determined by physically measuring the depth of the sediment above the bedrock. Madagascar mangroves showed a range of 324 Mg ha^{-1} to 517 Mg ha^{-1} considering a soil carbon to 150 cm (Jones, et al. 2014).

7.5 Ecosystem Carbon Stock

The ecosystem carbon stock (i.e., the sum of all carbon pool densities) in the Zambezi River Delta, 374 Mg ha^{-1} to 621 Mg ha^{-1}, is within the range of reported mangrove forest estimates from other regions. In the Indo-West Pacific, reported carbon storage values range from 830 Mg C ha^{-1} to 1218 Mg C ha^{-1} (Donato, et al. 2011,Kauffman, et al. 2011,Donato, et al. 2012). Caribbean mangroves exhibit a wide range of total carbon stock, with published values ranging from 287 Mg C ha^{-1} to 1131 Mg C ha^{-1} (Adame, et al. 2013,Kauffman, et al. 2014). Mangrove ecosystem carbon stocks in China range from 213 Mg C ha^{-1} to 443 Mg C ha^{-1} (Wang, et al. 2013). It is important to remember however, that these are ranges and that the sampling approaches are not consistent amongst studies (e.g., sampling intensity and soil depth considered).

Despite the differences in the magnitude of the various ecosystem carbon stock estimates, the relative contribution of the various components is similar throughout published studies and aligns with the results from this research. AGB accounts for about from 16% to 23% of total ecosystem carbon, while BGB contributes 8% to 16% of the total (Kauffman, et al. 2011,Donato, et al. 2012). The soil carbon pool is always the dominant component of the ecosystem carbon stock, with contributions being reported from 62% to 99% of the total (Donato, et al. 2012,Kauffman, et al. 2014,Jones, et al. 2014).

7.6 Carbon Inventory

In contrast to many synoptic studies, the purpose of this research was specifically to inventory the carbon pools in the Zambezi River Delta. Most mangrove carbon studies to date have not designed to assess a specific resource area and therefore cannot be considered as a designed inventory. A stratified random sampling design is one that is commonly used in forest inventories. Stratification can produce estimates with increased precision compared with simple random sampling, especially when the variable used to define the strata is highly correlated with the outcome being measured (US EPA 2002), as is the case with canopy height (stratification variable) and biomass (measured outcome).

The UN REDD+ program has specific guidance regarding acceptable levels of uncertainty and asks for a precision of a 95% confidence interval equal to or less than 15% of the recorded estimate. Our sampling design allowed us to achieve a precision of a 95% confidence interval equal to 6% of our ecosystem carbon stock estimate, well within the REDD+ guidelines. This precision is a direct result of our inventory approach, the stratified random sampling design, and high quality field and laboratory data.

There is an important consideration that was not included in our error propagation. Our estimates of uncertainty are based on the inventory boundary. However there is uncertainty associated with the mangrove area that we didn't take into account. Our area is based on just one of several remote sensing data sets and analytical approaches, some of which provide very different estimates of area (Table 3.1). However, given the relatively low variation in the measurements within the survey area, it's quietly likely that the reported values will not vary substantively if the survey boundary is revised.

8 Conclusion

The main objectives of this Project were to provide policy-relevant information necessary to establish a baseline for REDD+, to build capacity in Mozambique for climate change mitigation and adaptation programs, and to measure the carbon contained within the Zambezi River Delta mangrove forests.

Capacity building was realized with 4 institutions:

- Universidade de Eduardo Mondlane (UEM)
- World Wildlife Fund- Mozambique (WWF)
- Government of Mozambique- Ministry of Agriculture, National Directorate of Land Forestry (DNTF)
- Government of Mozambique- Ministry of the Environment-Center for Coastal and Marine Environment Research (CEPAM)

Students from UEM and employees from each of the other above institutions benefitted from the two field methods training sessions held in October 2012 and September 2013. The relationships established in these trainings have already led to additional collaborative interactions, including the loaning of field equipment for other projects and technical advice and recommendations on field approaches and methods.

Two field campaigns were conducted, October 2012 and September 2013, to complete the required field sampling to inventory carbon pools in intact mangrove forests within the Zambezi River Delta. Project methods, modified from standard, internationally-recognized protocols, were consolidated into a field manual that was distributed to field crews for training and reference purposes. This manual is being expanded to create a more comprehensive document that discusses not only the field methods themselves, but also sampling design and data processing and analyses. The revised manual will be available by the end of 2014.

The Project also demonstrated the effective application of the canopy height as the basis for stratification and forest classification. The identified canopy height classes reflected variations in stand density and height that resulted in corresponding differences in biomass and carbon estimates. This approach to delineating and "classifying" the mangrove area is simple but effective and would be easy to replicate in other global mangrove areas, regardless of spatial extent or species composition.

The Project estimated a total ecosystem carbon stock, including all biomass/vegetation pools, as well as soil, for the Zambezi River Delta of 1.4 x 10^7 Mg of carbon. This storage value is well within range of carbon stocks reported for mangroves within Africa, as well as on other continents. The results also contribute to the body of literature that suggests that soils are the most significant pool in mangrove carbon storage, with soil contributions ranging from 45% to 73% of the ecosystem carbon pool.

9 Recommendations

The following recommendations are intended as guidance to ensure that the data and knowledge developed from this project are available as the GoM develops its REDD+ strategy and implements a national mangrove inventory. These recommendations are also intended to avail project information to other scholars, researchers, or natural resource management professionals. Finally, suggestions are provided to capitalize on the foundation developed through this project.

a) Incorporate Data into the National Forest Inventory and MRV system-

The project data provide the first comprehensive assessment of a large tract of mangrove forest in Mozambique. Accordingly, this data should be incorporated into the national forest inventory and MRV system[9]. The findings from this project should also be used by GoM to inform the design and implementation of the mangrove inventory that is planned for the coming years. While follow-on capacity building is needed for GoM and partners, available protocols on plot design, layout and measurements will enhance the efficiency and accuracy of any new work. Additional research would be highly valuable in other deltaic systems, as well as bay mangrove areas, to further refine the methodology and estimation tools.

b) Establish Permanent Monitoring Plots –

A subset of the plots used in this project should be established as permanent monitoring locations; by establishing permanent monitoring plots, it would be possible to assess the change in forest composition and structure over time. The selected plots[10] should be chosen from each of the canopy height classes to ensure that the full spectrum of mangrove stand conditions is included. The plot centers of each of the subplots within the selected plots should be witnessed by installing a permanent stake, and marking the trees near plot center. If this action is performed by the end of 2015, the locations should be quite evident from the marking tape used in 2013.

c) Conduct a Change Assessment of Mangroves –

Documenting both the natural and anthropogenic change in mangrove area is fundamental to developing a REDD+ strategy. This assessment is needed for the Zambezi River Delta since the project only considered the carbon pools in intact forest stands, as well as other areas of the

[9] It is likely that computed results from the project data will be required.

[10] The coordinates of the center subplot are provided as part of the project documents, along with a GIS shape file.

country. The recommended approach would use a combination of field monitoring stations, field reconnaissance, and use of high resolution remote sensing data. The goal of the monitoring would be to develop an estimate of the annual rate of change in mangrove area along the coast of Mozambique.

10 References

1. FAO. 2007 The world's mangroves 1980-2005. Rome.
2. Kathiresan, K. and Bingham, B.L. 2001 Biology of Mangroves and Mangrove Ecosystems. *Advances in Marine Biology*, **40**, 81-251.
3. Krauss, K.W., Lovelock, C.E., McKee, K.L., López-Hoffman, L., Ewe, S.M.L. and Sousa, W.P. 2008 Environmental drives in mangrove establishment and early development: A review. *Aquatic Botany*, **89**, 105-127.
4. Hogarth, P.J. 2007 *The Biology of Mangroves and Seagrasses*. Second Edition edn. Oxford University Press.
5. Giri, C., Ochieng, E., Tieszen, L.L., Zhu, Z., Singh, A., Loveland, T. *et al.* 2011 Status and distribution of mangrove forest of the world using earth observation satellite data. *Global Ecology and Biogeography*, **20** (1), 154-159.
6. IPCC. 2013 The Physical Science Basis. Contribution of Working Group I to the Fifth Assessment Report of the Intergovernmental Panel on Climat Change. United Kingdom and New York, NY, USA, p. 1535.
7. van der Werf, G.R., Morton, D.C., DeFries, R.S., Olivier, J.G.J., Kasibhatla, P.S., Jackson, R.B. *et al.* 2009 CO_2 emisions from forest loss. *Nature Geoscience*, **2**, 737-738.
8. Gullison, R.E., Frumhoff, P.C., Canadell, J.G., Field, C.B., Nepstad, D.C., Hayhoe, K. *et al.* 2007 Tropical Forests and Climate Policy. *Science*, **316**, 985-986.
9. Kollmuss, A.A., Zink, H. and Polycarp, C. 2008 Making Sense of the Voluntary Carbon Market: A Comparison of Carbon Offset Standards.
10. Adame, M.F., Kauffman, J.B., Medina, I., Gamboa, J.N., Torres, O., Caamal, J.P. *et al.* 2013 Carbon Stocks of Tropical Coastal Wetlands within the Karstic Landscape of the Mexican Caribbean. *PLoS ONE*, **8** (2), e56569.
11. Murdiyarso, D., Kauffman, J.B., Warren, M., Pramova, E. and Hergoualc'h, K. 2012 Tropical wetlands for climate change adaptation and mitigation science and policy imperatives with special reference to Indonesia *No. Working Paper 91*. Center for International Forestry Research.
12. UN-REDD. 2011 The UN-REDD Programme Strategy 2011-2015. United Nations collaborative initiative on Reducing Emissions from Deforestation and Forest Degradation (REDD+) in developing countries.
13. Donato, D.C., Kauffman, J.B., Murdiyarso, D., Kurnianto, S., Stidham, M. and Kanninen, M. 2011 Mangroves amongst the most carbon-rich forests in the tropics. *Nature Geoscience*, **4** (5), 293-297.
14. King, L. 2012 Including mangrove forests in REDD+. *Notes From The Field*. CDKN.
15. Kauffman, J.B., Heider, C., Cole, T.G., Dwire, K.A. and Donato, D.C. 2011 Ecosystem Carbon Stocks of Micronesian Mangrove Forests. *Wetlands*, **31**, 343-352.
16. Kristensen, E., Bouillon, S., Dittmar, T. and Marchand, C. 2008 Organic carbon dynamics in mangrove ecosystems: A review. *Aquatic Botany*, **89**, 201-219.
17. Fatoyinbo, T.E. and Simard, M. 2013 Height and biomass of mangroves in Africa from ICESat/GLAS and SRTM. *International Journal of Remote Sensing*, **34** (2), 668-681.
18. Chevallier, R. 2013 Balancing Development and Coastal Conservation: Mangroves in Mozambique. *Governance of Africa's Resources Programme*. South African Institute of International Affairs
19. Barbosa, F.M.A., Cuambe, C.C. and Bandeira, S.O. 2001 Status and distribution of mangroves in Mozambique. *South African Journal of Botany*, **67**, 393-398.
20. Taylor, M., Ravilious, C. and Green, E., P. 2003 Mangroves of East Africa. UNEP World Conservation Monitoring Centre. United Kingdom.

21. Beilfuss, R.D., Moore, D., Bento, C. and Dutton, P. 2001 Patterns of Vegetation Change in the Zambezi Delta, Mozambique. *Program for the Sustainable Management of Cahora Bassa Dam and the Lower Zambezi Valley*.
22. Beentje, H. and Bandeira, S. 2007 *Field Guide to the Mangrove Trees of Africa and Madagascar*. Kew Publishing: Royal Botanic Gardens, Kew.
23. Bandeira, S.O., De Silva, R.P., Paula, J., Macia, A., Hernroth, L., Guissamulo, A.T. *et al.* 2002 Marine Biological Research in Mozambique: Past, Present and Future. *Ambio*, **31** (7/8), 606-609.
24. Hatton, J.C. and Couto, A.L. 1992 The effect of coastline changes on mangrove community structure, Portuguese Island, Mozambique. *Hydrobiologia*, **247**, 49-57.
25. Mozambique, R.o. 2009 National Report on Implementation of the Convention on Biological Diversity in Mozambique. Maputo, Mozambique.
26. WWF. 2011 Wet Carbon- Conserving Mangroves in the Zambezi Delta, Mozambique. In *Project Idea Note*, WWF Mozambique Country Programme Office, Maputo, Moz.
27. Ferreira, M.A., Andrade, F., Bandeira, S.O., Cardoso, P., Mendes, R.N. and Paula, J. 2009 Analysis of cover change (1995-2005) of Tanzania/Mozambique trans-boundary mangroves using Landsat imagery. *Aquatic Conservation: Marine and Freshwater Ecosystems*, **19**, S38-S45.
28. Fatoyinbo, T.E., Simard, M., Washington-Allen, R.A. and Shugart, H.H. 2008 Landscape-scale extent, height, biomass, and carbon estimation of Mozambique's mangrove forests with Landsat ETM+ and Shuttle Radar Topography Mission elevation data. *Journal of Geophysical Research*, **113**, G02S06.
29. Bandeira, S.O., Macamo, C.C.F., Kairo, J.G., Amade, F., Jiddawi, N. and Paula, J. 2009 Evaluation of mangrove structure and condition in two trans-boundary areas in the Western Indian Ocean. *Aquatic Conservation: Marine and Freshwater Ecosystems*, **19**, S46-S55.
30. Timberlake, J. 2000 Biodiversity of the Zambezi Basin. Biodiversity Foundation for Africa. Bulawayo, Zimbabwe.
31. Beilfuss, R.D. and Santos, D.d. 2001 Patterns of Hydrological Change in the Zambezi Delta, Mozambique. *Program for the Sustainable Management of Cahora Bassa Dam and the Lower Zambezi Valley*.
32. Davies, B.R., Beilfuss, R.D. and Thoms, M.C. 2000 Cahora Bassa retrospective, 1974-1997: effects of flow regulation on the Lower Zambezi River. *Verhandlungen des Internationalen Verein Limnologie*, **27**, 1-9.
33. Bank, T.W. 2010 State of the Basin. *The Zambezi River Basin: A Multi-Sector Investment Opportunities Analysis*. The World Bank.
34. Timberlake, J. 1998 Biodiversity of the Zambezi Basin Wetlands: Review and Preliminary Assessment of Available Information. The Zambezi Society/Biodiversity Foundation for Africa.
35. Coleman, J. 2004 The Zambezi Delta. (May 23, 2014, 2014).
36. Hoguane, A.M. 2007 Perfil Diagnóstico da Zona Costeira de Moçambique. *Revista de Gestão Costeira Integrada*, **7** (1), 69-82.
37. Bento, C.M., Beilfuss, R.D. and Hockey, P.A. 2007 Distribution, structure and simulation modelling of the Wattled Crane population in the Marromeu Complex of the Zambezi Delta, Mozambique. *Ostrich-Journal of African Ornithology*, **78** (2), 185-193.
38. Tweddle, D. 2013 Lower Zambezi. (5/20/2014, 2014).
39. Vilankulos, M. and Marquez, M.R. 2000 Physical characterization of the coastal zone of mangrove areas in the districts of Dondo and Marromeu, Sofala, based on interpretation of aerial photographs. *Baseline data and evaluation procedures for the formulation of Mangrove Resources Management Plan in the northern part of Sofala Province*. Direcçao Nacional de Florestas e Fauna Bravia. Maputo.

40. Smith, T.J.I. 1992 Forest Structure. In *Tropical mangrove ecosystems.* A.I. Robertson and D.M. Alongi (eds.), American Geophysical Union, Washington, D.C., pp. 101-136.
41. Moll, E.J. and Werger, M.J.A. 1978 Mangrove Communities. In *Biogeography and ecology of Southern Africa.* M.J.A. Werger and A.C. van Bruggen (eds.), Dr. W. Junk Publishers, The Hague.
42. Rafael, J., Bosire, J.O. and Bandeira, S.O. 2011 Coastal climate change mitigation and adaptation through REDD+ carbon programs in mangroves in Mozambique: Mangrove classification for the Zambezi Delta. WWF.
43. Tang, W., Feng, W., Wang, Y., Jia, M., Deng, J. and Zuo, H. 2013 Development of Spatial Decision Support System for Mangrove Inventory in the Zambezi Delta, Mozambique. UNC-Charlotte.
44. Kauffman, J.B. and Donato, D.C. 2012 Protocols for the measurement, monitoring and reporting of structure, biomass and carbon stocks in mangrove forests. Center for International Forestry Research. Bogor, Indonesia.
45. Van Wagner, C.E. 1968 The Line Intersect Method in Forest Fuel Sampling. *Forest Science*, **14** (1), 20-26.
46. Brown, J.K. 1971 A Planar Intersect Method for Sampling Fuel Volume and Surface Area. *Forest Science*, **17** (1), 96-102.
47. Komiyama, A., Poungparn, S. and Kato, S. 2005 Common allometric equations for estimating the tree weight of mangroves. *Journal of Tropical Ecology*, **21**, 471-477.
48. Bosire, J.O., Bandeira, S.O. and Rafael, J. 2012 Coastal climate change mitigation and adaptation through REDD+ carbon program in mangroves in Mozambique: Pilot in the Zambezi Delta. WWF, p. 27.
49. World Agroforestry Center. Wood Density Database. 2013).
50. Komiyama, A., Havanond, S., Srisawatt, W., Mochida, Y., Fujimoto, K., Ohnishi, T. *et al.* 2000 Top/root biomass ratio of a secondary mangrove (*Cerips tagal* (Perr.) C.B. Rob.) forest. *Forest Ecology and Management*, **139** (1), 127-134.
51. Komiyama, A., Ogino, K., Aksornkoae, S. and Sabhasri, S. 1987 Root Biomass of a Mangrove Forest in Southern Thailand. 1. Estimation by the Trench Method and the Zonal Structure of Root Biomass. *Journal of Tropical Ecology*, **3** (2), 97-108.
52. Thomas, G.W. 1996 Soil pH and soil acidity. In *Methods of Soil Analysis: Part 3-Chemical Methods*, Soil Science Society of America, Madison, Wisconsin, pp. 475-490.
53. 2010 Organic Elemental Analysis of Soils- Understanding the Carbon-Nitrogen Ratio. P. Elmer (ed.), Perkin Elmer, Waltham, MA, USA.
54. Cormack, R. 1988 Statistical challenges in the environmental sciencesL a personal view. *Journal of the Royal Statistical Society. Series A (Statistics in Society)*, 201-210.
55. Nusser, S., Breidt, F. and Fuller, W. 1998 Design and estimation for investigating the dynamics of natural resources. *Ecological Applications*, **8** (2), 234-245.
56. Feller, I.C. and Sitnik, M. 1996 Mangrove Ecology Workshop Manual. Smithsonian Institution, Washington, DC.
57. Janzen, D.H. 1985 Mangroves: Where's the Understory? *Journal of Tropical Ecology*, **1** (1), 89-92.
58. Donato, D.C., Kauffman, J.B., Mackenzie, R.A., Ainsworth, A. and Pfleeger, A.Z. 2012 Whole-island carbon stocks in the tropical Pacific: Implications for mangrove conservation and upland restoration. *Journal of Environmental Management*, **97**, 89-96.
59. Kauffman, J.B., Heider, C., Norfolk, J. and Payton, F. 2014 Carbon stocks of intact mangroves and carbon emissions arising from their conversion in the Dominican Republic. *Ecological Applications*, **24** (3), 518-527.
60. Slim, F.J., Gwada, P.M., Kodjo, M. and Hemminga, M.A. 1996 Biomass and Litterfall of *Ceriops tagal* and *Rhizophora mucronata* in the Mangrove Forest of Gazi Bay, Kenya. *Marine and Freshwater Research*, **47** (8), 999-1007.

61. Kirui, B.K. 2006 *Allometric Relations for Estimating Aboveground Biomass of Naturally Growing Mangroves, Avicennia marina Forsk (Vierh). and Rhizophora mucronata Lam. along the Kenya Coast.* Master of Science Degree in Natural Resources Management, Egerton University.
62. Cohen, R., Kaino, J., Okello, J.A., Bosire, J.O., Kairo, J.G., Huxam, M. *et al.* 2013 Propagating uncertainty to estimates of above-ground biomass for Kenyan mangroves: A scaling procedure from tree to landscape level. *Forest Ecology and Management*, **310**, 968-982.
63. Fromard, F., Puig, H., Mougin, E., Marty, G., Betoulle, J.L. and Cadamuro, L. 1998 Structure, above-ground biomass and dynamics of mangrove ecosystems: new data from French Guiana. *Oecologia*, **115**, 39-53.
64. Komiyama, A., Ong, J.E. and Poungparn, S. 2008 Allometry, biomass, and productivity of mangrove forests: A review. *Aquatic Botany*, **89**, 128-137.
65. Wang, G., Guan, D., Peart, M.R., Chen, Y. and Peng, Y. 2013 Ecosystem carbon stocks of mangrove forest in Yingluo Bay, Guangdong Province of South China. *Forest Ecology and Management*, **310**, 539-546.
66. Jones, T.G., Ratsimba, H.R., Ravaoarinorotsihoarana, L., Cripps, G. and Bey, A. 2014 Ecological Variability and Carbon Stock Estimates of Mangrove Ecosystems in Northwestern Madagascar. *Forests*, **5**, 177-205.
67. U.S.E.P.A. 2002 Guidance for Choosing a Sampling Design for Environmental Data Collection (EPA QA/G-5S). U.S. Envrionmental Protection Agency.

11 Project Bibliography

1. Rafael, J., J. Bosire, S. Bandeira. 2011. Coastal climate change mitigation and adaptation through REDD+ Carbon programs in mangroves in Mozambique: Mangrove classification for the Zambezi Delta. WWF. 7 pg.
2. Bosire J. O., Bandeira S., Rafael J. 2012. Coastal climate change mitigation and adaptation through REDD+ Carbon programs in mangroves in Mozambique: Pilot in the Zambezi Delta. Determination Of carbon stocks through localized allometric equations component. WWF. 27 pg.
3. West Indian Ocean Mangrove Network. 2012. Proceedings of the East Africa Mangrove Workshop. Maputo, October, 2012.
4. Trettin, C., J. Ko, S. Nazerali, D. Nicolau, S. Bandeira, C. Macamo. Assessing Mangrove Carbon Pools in the Zambezi Delta. A presentation to WWF. 29 January 2013.
5. Trettin, C. Zambezi Overview. A presentation to USAID. 28 February 2013.
6. Trettin, C. Assessment of Carbon Pools within Mangrove Forests on the Zambezi Delta, Mozambique: Progress Report 1- 2012 Field Mission. 26 March 2013.
7. Tang, W., W. Feng, T. Wang, M. Jia, J. Deng, H. Zuo. Development of Spatial Decision Support System for Mangrove Inventory in the Zambezi Delta, Mozambique: A Report Submitted to Dr. Carl C Trettin. University of North Carolina Charlotte: Center for Applied GIScience. 4 June 2013. [Project Report]
8. Stringer, C., C. Trettin. Assessment of Carbon Pools within Mangrove Forests on the Zambezi Delta, Mozambique: Progress Report 2- 2012 Field Mission. 5 August 2013.
9. Trettin, C.C., C.E. Stringer, S. Bandeira, C. Macamo, J. Bosire, D. Nicolau, R. Mabunda, and J. Rafael. 2013. Assessing Carbon Stocks in Mangroves within the Zambezi Delta, Mozambique. West Indian Ocean Marine Science Association 8th Scientific Symposium. Maputo, Mozambique.
10. Trettin, C.C., J. Ko, C.E. Stringer, and M. Patrick. 2013. East Africa Regional Mangrove Carbon Project: Carbon Dynamics- the Foundation of Ecosystem Services in Mangroves in East Africa. West Indian Ocean Marine Science Association 8th Scientific Symposium. Maputo, Mozambique.
11. Mission Reports:
    a. Sept. 2012: Field mission report (Trettin & Sanders)
    b. Oct. 2012. Workshop mission report (Ko & Trettin)
    c. April 2013: Due diligence mission, project planning (Ko & Trettin)
    d. Sept. 2013: Field mission report (Trettin & Stringer)